PERGAMON

Quaternary Science Reviews 21 (2002) 203–231

QSR

Sea-level changes at the LGM from ice-dynamic reconstructions of the Greenland and Antarctic ice sheets during the glacial cycles

Philippe Huybrechts*

Alfred-Wegener-Institut für Polar-und Meeresforschung, Postfach 120161, D-27515 Bremerhaven, Germany

Received 26 February 2001; accepted 23 July 2001

Abstract

New experiments were performed with three-dimensional thermomechanical models of the Greenland and Antarctic ice sheets to simulate their behaviour during the glacial cycles, to reconstruct their thickness and extent at the Last Glacial Maximum (LGM), and to estimate their glacio-eustatic contribution to the global sea-level stand. The calculations used improved ice-dynamic and isostatic treatments, updated datasets on higher grid resolutions, and refined climatic treatments based on newly calibrated transfer functions between ice core records and climatic perturbations. Results are discussed from a reference run with standard parameters that is compared with available glacial-geological observations, and from a series of sensitivity experiments focusing on isostatic adjustment, thermomechanical coupling, climatic forcing, mass-balance changes, and basal melting rates and viscosity changes of Antarctic ice shelves. For the Antarctic ice sheet, we find that volume changes are closely linked with grounding line changes of the West Antarctic ice sheet. At the LGM, the grounding line extended close to the continental shelf break almost everywhere. Ice over central East Antarctica was generally thinner than today and varied mainly in accordance with accumulation fluctuations. For the Greenland ice sheet, melting is important only during interglacial periods and the most sensitive period concerns the size of the ice sheet during the Eemian. At the LGM, the Greenland ice sheet extended beyond the present coastline to cover at least the inner continental shelf and thinned by up to several hundred meters in central areas. For a plausible range of parameters, the experiments indicate that at the time of maximum sea-level depression (21 kyr BP), the Antarctic ice sheet contributed 14–18 m to the sea-level lowering, and the Greenland ice sheet 2–3 m, significantly less than the older CLIMAP reconstructions. Whereas both ice sheets were at 21 kyr BP close to their maximum extent, the experiments also indicate that their maximum volumes were reached only by 16.5 kyr BP (Greenland) and 10 kyr BP (Antarctica), equal to an additional sea-level lowering of, respectively, 0.4 and 3.7 m. Holocene retreat was essentially complete by 5 kyr BP in Greenland, but is found to still continue today in West Antarctica before reversing to growth during the next millenium. The models were found to reproduce gross features of the ice sheet's history since the LGM in reasonably good agreement with available glacial-geological data, although observational control on ice thickness changes remains very limited.

1. Introduction

The Greenland and Antarctic ice sheets constitute a vital component of the global water balance during the glacial cycles. They are the only two large ice masses that survived the last glacial–interglacial transition, enabling to study them today and construct a baseline against which models and hypotheses can be tested. Together, their current volume contains enough ice to raise global sea level by almost 70 m, of which 61 m would derive from the Antarctic ice sheet (Huybrechts et al., 2000) and 7 m from the Greenland ice sheet (Letréguilly et al., 1991a). Major issues concern how much additional water was locked up in these ice sheets at the Last Glacial Maximum (LGM), when this maximum occurred, and over which period the ice was released back into the oceans. This problem bears directly on the amount of ice stored elsewhere on the globe as the total eustatic sea-level depression is rather well constrained to have been between ca. 125 and 135 m (Fairbanks, 1989; Yokoyama et al., 2000).

The majority of ice at the LGM was contained in the ice sheets of Laurentia and Fennoscandia, but their combined estimated volume falls far short of the required ~130 m in many assessments, in particular in

*Corresponding author. Tel.: +49-471-4831-1194; fax: +49-471-4831-1149.

E-mail address: phuybrechts@awi-bremerhaven.de (P. Huybrechts).

0277-3791/02/$ - see front matter
PII: S0277-3791(01)00082-8

studies based on rebound data (e.g. Nakada and Lambeck, 1988; Tushingham and Peltier, 1991; Peltier, 1994). Hence, there is a problem where the remainder of the ice was stored, and there has been a tendency to put as much as 37 m in Antarctica (Nakada and Lambeck, 1988) and 6 m in Greenland (Tushingham and Peltier, 1991) to explain the total sea-level change. Other lines of evidence indicate that the polar ice sheets contained much less ice at the LGM, and thus that the 'missing water' must have come from elsewhere (Andrews, 1992). For instance, Colhoun et al. (1992) used the ages and elevations of raised beaches in the Ross Embayment and on Eastern Antarctica to find only a 0.5–2.5 m Antarctic contribution to the postglacial sea-level rise, even less than the 6–13 m obtained from an attempt to reconcile glacial-geological, glacio-isostatic, modelling, and ice-core data (Bentley, 1999). Early glaciological modelling of the Greenland ice sheet (Letréguilly et al., 1991b) estimated the Greenland contribution to be about 0.8 m, close to the minimum CLIMAP estimate of 0.7 m (Denton and Hughes, 1981), but other models suggest a higher contribution (Marshall and Cuffey, 2000). An additional problem is that all of the ice sheets may not have peaked synchronously at the time of maximum sea-level depression, which is generally believed to have occurred between 23 and 19 kyr BP (Clark and Mix, 2000).

In this paper, the problem of Antarctica and Greenland's contribution to global sea levels is tackled by glaciological modelling of their history over the last few glacial cycles. These long simulation periods are required to cover the long response time scales of the polar ice sheets (10^2–10^4 yr) so that their maximum at the end of the last ice age is unlikely to have corresponded to an equilibrium state. The time-dependent three-dimensional thermomechanical models are based on mathematical relations that govern ice accumulation/loss, the flow of ice, and the interaction with the underlying bedrock. Such models have an important role to integrate the various pieces of palaeoclimatic information, and to establish the ice thickness distribution over time, which in general cannot be inferred from field data as the ice sheets left little direct evidence of their height. Constraints on reconstructed past volumes are then mainly provided by comparison with glacial-geological data for their maximum extent and their timing of Holocene retreat.

First glaciological model studies simulating the polar ice sheets during the glacial cycles were performed a decade ago (Huybrechts, 1990; Letréguilly et al., 1991b). Since then, similar studies documented various other aspects of the Late Quaternary history of the Greenland (Huybrechts, 1996; Weis et al., 1996; Greve, 1997; Ritz et al., 1997; van de Wal, 1999; Cuffey and Marshall, 2000; Marshall and Cuffey, 2000) and Antarctic ice sheets (Le Meur and Huybrechts, 1996; Ritz et al., 2001). Typical ranges in these studies of the LGM contribution to the global sea-level depression were 8–16 m for Antarctica and 1–2.5 m for Greenland, much less than the CLIMAP estimates of, respectively, 24.7 and 6.4 m (maximum) obtained for a rock-ice density ratio of 4 and complete isostatic equilibrium (Denton and Hughes, 1981). The experiments discussed in this paper are based on the upgraded ice-dynamic and bedrock models described in Huybrechts and de Wolde (1999), but differ by using new higher-resolution datasets for Antarctica, a better treatment of mass-balance components based on improved observations and new temperature-isotope transfer functions, and new forcing time series. Sections 2 and 3 present the ice-sheet and mass-balance models and discuss the improvements with respect to previous work. Simulations of the Antarctic and Greenland ice sheets are presented in Sections 4 and 5, and deal with the model forcing, the results from a reference experiment with standard parameter values, a comparison with available field data, and the results of a series of sensitivity experiments in which crucial parameters are varied within plausible ranges of uncertainty. The latter provides the envelope of the likely response of the Greenland and Antarctic ice sheets during the glacial cycles based on our best current knowledge of ice dynamics and environmental forcing. As such, these experiments review the current state of polar ice-sheet modelling. The emphasis of the presentation is on ice-sheet behaviour during the LGM and its subsequent Holocene retreat and on implied equivalent sea-level changes, but evolution curves are displayed for the last four (Antarctica) and two (Greenland) glacial cycles, respectively.

2. The ice sheet models

The numerical models freely simulate ice-sheet thickness and extent in response to prescribed changes of climatic conditions (sea level, surface temperature, snow accumulation, and ice ablation). The entire model consists of three main components which, respectively, describe the ice flow, the solid Earth response, and the mass balance at the ice–atmosphere and ice–ocean interfaces.

The ice-dynamic and isostatic components of the models are identical to those described in Huybrechts and de Wolde (1999), to which the interested reader is referred for a full account of assumptions and formulations. The core of the model is the simulation of thermomechanical flow for grounded ice, which results from both internal deformation and sliding over the bed in places where the temperature reaches the pressure melting point. Only shearing in horizontal planes is considered and longitudinal stress effects are ignored. The rate factor in Glen's flow law depends primarily on

temperature, but also allows for the different ice stiffnesses of Holocene and ice-age ice as established in Greenland ice cores. Therefore a full three-dimensional calculation of ice temperature is performed simultaneously with the velocity calculations, and a procedure is adopted to track the depth of the Holocene/Wisconsin boundary in the Greenland model. Heat conduction is considered in an underlying bedrock slab of 4 km thickness. The geothermal heat flux is $54.6\,\mathrm{m\,W\,m^{-2}}$ for Antarctica and $48.3\,\mathrm{m\,W\,m^{-2}}$ for Greenland, somewhat higher than in previous studies but not crucial in the context of this paper.

A major distinction between the Greenland and Antarctic ice-sheet models concerns the treatment of the grounded ice margin. The Antarctic model explicitly includes a dynamic ice shelf to enable interaction with the ocean and migration of the grounding line. The latter separates grounded ice from floating ice, and is instrumental to determine the evolving shape of in particular the West Antarctic ice sheet. Having a melt margin on land or a calving margin close to the coastline for most of its glacial history, ice shelves played only a minor role for the dynamics of the Greenland ice sheet, and are therefore not included in the Greenland model. Instead, the model predicts a coastline from the contemporaneous sea-level stand and the local bedrock height, beyond which all ice is removed as calf ice. The treatment allows the ice sheet to expand and contract over the continental shelf within limits provided by the current coastline and a maximum extent reconstructed from geological data, insofar the surface mass-balance permits it. No attempts are made to predict the position of the marine margin from a self-consistent treatment of calving dynamics, because a convincing calving relation does not exist. Calving fronts of Antarctic ice shelves are not explicitly traced either, but this has negligible effect on the position of the grounding-line, which is of main interest.

In common with the current generation of three-dimensional ice-sheet models, the models used in this study do not include any of the physics specific to fast-flowing outlet glaciers or ice streams. That is partly a resolution problem, since these features cannot be sufficiently resolved on the 20 km grids employed by both models, but also the nature of the force balance and the flow law at lateral and basal boundaries of such fast-flowing features is poorly known (Van der Veen, 1999). Likewise, any differentiation in bed characteristics other than freezing/thawing is ignored and processes related to deformation of water-saturated weak sediments are not treated. The effects of these simplifications are probably most relevant for the West Antarctic ice sheet (WAIS), especially in the Ross Basin, where the present outflow mainly occurs through distinct ice streams whose beds are believed to consist of a thick sequence of soft sediment layers extending all the way to the continental break (Anderson, 1999).

Isostasy needs to be considered for its effect on bed elevation near grounding lines and marginal ablation zones, where it matters most for ice-sheet dynamics, and because isostasy enables ice sheets to store 25–30% more ice than evident from their surface elevation alone. The bedrock adjustment model consists of a viscous asthenosphere, described by a single isostatic relaxation time, which underlies a rigid elastic plate (lithosphere). In this way, the isostatic compensation takes into account the effects of loading changes within an area several hundred kilometers wide, giving rise to deviations from local isostatic equilibrium. The value for the flexural rigidity ($1\times10^{25}\,\mathrm{N\,m}$) corresponds to a lithospheric thickness of 115 km; the characteristic relaxation time for the asthenosphere is 3000 yr. Versions of the ice-sheet model have been developed that use a more sophisticated self-gravitating spherical visco-elastic earth model (Le Meur and Huybrechts, 1996, 1998), but the associated computational burden precludes running a large number of sensitivity experiments. However, for the simulation of the polar ice sheets over the glacial cycles the approach adopted here produces results close to those from a full visco-elastic treatment with mantle viscosities in the range $0.5\text{–}1.0\times10^{21}\,\mathrm{Pa\,s}$ and a lithosphere thickness of 100 km (Le Meur and Huybrechts, 1996), and is at the same time much more realistic than the local isostatic equilibrium/diffusive asthenosphere approach adopted in much of the older ice-sheet model studies. The loading takes into account contributions from both ice and ocean water within the respective grids, but ignores any ice loading changes beyond the Greenland and Antarctic continental areas.

The calculations are performed on detailed three-dimensional grids with 20 km horizontal resolution and 31 layers in the vertical for both ice sheets. Including a calculation of heat conduction in the bedrock, this gives rise to between 0.4 and 2.9×10^{6} grid nodes for Greenland and Antarctica, respectively. For Antarctica, it represents a doubling of the horizontal resolution with respect to earlier versions of the model, enabling to implement the upgraded data sets presented in Huybrechts et al. (2000). The grids are laid out over the usual polar stereographic map projections with standardparallel at 71°. The calculations account for the horizontal distortions of distance arising from the map projection.

3. The mass-balance treatment

The third component of the model is the mass balance, which represents the link between the ice sheet and the climate system (atmosphere and ocean). The treatment adopted in this study relies on techniques that have become commonplace in large-scale ice-sheet modelling. For the surface mass balance, a distinction

is made between the snowfall rate at the one hand and meltwater runoff at the other hand. Both are parameterized in terms of temperature, with surface temperature parameterizations following those presented in Huybrechts and de Wolde (1999). The precipitation rate is based on its present distribution and perturbed in different climates according to sensitivities derived from ice-core studies. This means that only the precipitation intensity can change, but not its pattern. Major changes in precipitation patterns were no doubt associated with the evolving Quaternary ice sheets on the northern hemisphere continents because of important changes in topography and atmospheric circulation. However, major effects beyond those already captured in the ice cores may have been less crucial for the Greenland ice sheet, where melting dominates the mass balance and the ice sheet had a rather similar shape for most of its late Quaternary history, and for most of the Antarctic ice sheet, where a strong dependence was established between precipitation rate and the saturated water vapour pressure at the condensation temperature above the surface inversion layer (Robin and de, 1977; Bromwich, 1988). As long as the ice sheets did not drastically change their dimensions, the assumption of a stationary precipitation pattern is probably the best one can do. It at least ensures that the present state is represented in the best possible way.

The melt-and-run-off model is based on the positive degree-day method. It takes into account ice and snow melt, the daily temperature cycle, random temperature fluctuations around the daily mean, and the subsequent retention and refreezing of meltwater. The model employed here is identical to the recalibrated version described in Janssens and Huybrechts (2000), with a meltwater retention treatment based on the capillary suction effect of the snowpack (Pfeffer et al., 1991). The same melt model is also implemented for Antarctica, but since summer temperatures remain generally below freezing, even for a few degrees warming, there is hardly any runoff from the grounded ice sheet at any time during the glacial cycles. Because of their very low surface slopes, it is further assumed that meltwater produced on the surface of the Antarctic ice shelves, if any, refreezes in situ at the end of the summer season, and therefore does not escape to the ocean. Below the ice shelves, a uniform melting rate is applied in which magnitude is linked to the temperature forcing, as explained further below.

4. Simulations of the Antarctic ice sheet

The main interest of this paper is on ice-sheet behaviour around the LGM, but the calculations were performed over the last 4 glacial cycles for which relevant climatic forcing is available. Spin-up over at least a full glacial cycle is required for the model to forget its initial start-up conditions. That especially applies to the temperatures in the deeper parts of the ice sheet, that are representative of average climatic conditions at the 100 kyr timescale. Long memory times of the coupled ice-sheet/bedrock system also imply that the state of the Antarctic ice sheet at the LGM is unlikely to correspond to a steady state, justifying the early startup date.

4.1. Model forcing

The model forcing deserves care because it dictates the chronology and magnitude of the response. Its components are driven by prescribed temperature and sea-level anomalies.

4.1.1. Temperature forcing

The temperature forcing consists of a temperature anomaly which is uniformly applied over the grid at 100-yr intervals, and from which changes in surface temperature, precipitation rate, and basal melting rate are estimated:

$$\Delta T_{\mathrm{VA}}(t) = a\Delta T_{\mathrm{VS}}(t) - \Delta T_{\mathrm{VC}}(t), \tag{1}$$

where $\Delta T_{\mathrm{VS}}(t)$ is the Vostok surface temperature change derived from the deuterium record for the standard spatial temperature/isotope gradient of 0.166°C per ‰δD (Petit et al., 1999), a is a constant to allow scaling of the forcing in the experiments ($a = 1$ in the standard case), and ΔT_{VC} is a term to correct for the change of the altitude of the Vostok region (Fig. 1). The latter term is equal to the Vostok elevation changes in the reference experiment (relative to present), multiplied by the central Antarctic surface atmospheric lapse rate of $-0.014285\,^{\circ}\mathrm{C\,m^{-1}}$ (Fortuin and Oerlemans, 1990). The correction term is roughly in phase with the Vostok record itself, but has an amplitude that is only 10–20% of the original signal, and is therefore a relatively minor correction. The corresponding elevation changes are between +50 and –150 m during the last 4 glacial cycles, implying corrections to the Vostok surface temperature record of between +0.7°C and –2°C, respectively.

4.1.2. Precipitation forcing

Precipitation changes above the Antarctic ice sheet are estimated as in previous model versions following relations suggested in Lorius et al. (1985):

$$T_{\mathrm{I}}(t) = 0.67T_{\mathrm{S}}(t) + 88.9, \tag{2}$$

$$P_{\mathrm{A}}[T_{\mathrm{I}}(t)] = P_{\mathrm{A}}[T_{\mathrm{I}}(\mathrm{present})]\exp\left\{22.47\left[\frac{T_0}{T_{\mathrm{I}}(\mathrm{present})} - \frac{T_0}{T_{\mathrm{I}}(t)}\right]\right\}\left\{\frac{T_{\mathrm{I}}(\mathrm{present})}{T_{\mathrm{I}}(t)}\right\}^2, \tag{3}$$

where T_{I} (in K) is the mean annual temperature above the surface inversion layer, T_{S} (in K) the mean annual

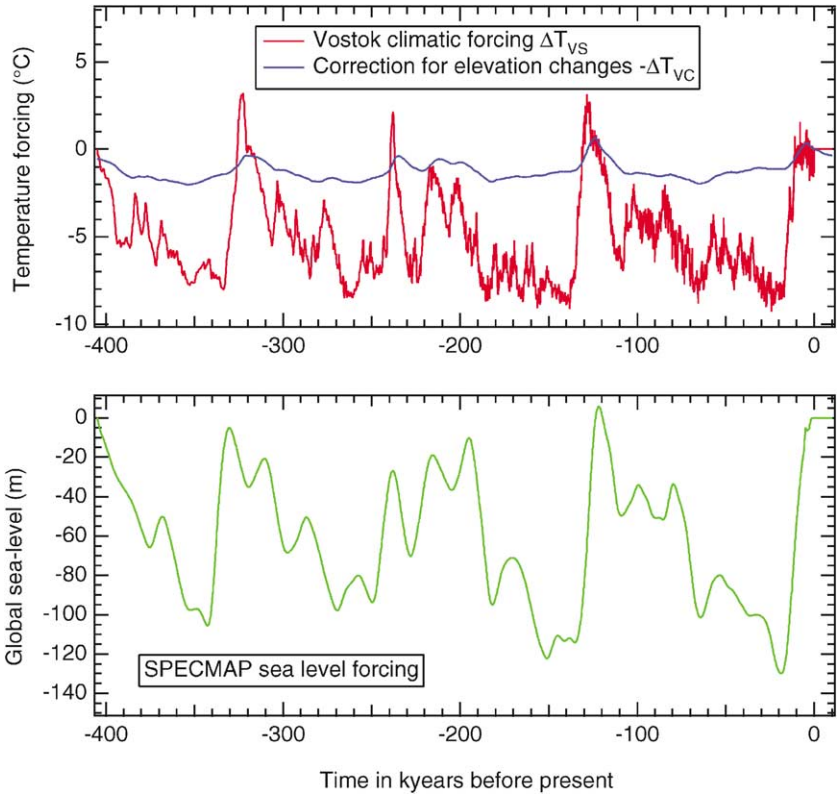

Fig. 1. Climatic (upper panel) and sea-level (lower panel) forcing used to reconstruct the history of the Antarctic ice sheet over the last four glacial cycles. Also shown is the correction term for elevation changes of the Vostok region in the reference experiment (A0) during the same time period.

surface temperature, P_A [T_I(present)] the present precipitation rate (in $m\,yr^{-1}$ of ice equivalent) and $T_0 = 273.16\,K$. The reference precipitation is taken from an amended Giovinetto map as presented in Huybrechts et al. (2000). The above treatment assumes that precipitation changes are proportional to the water vapour pressure gradient relative to the condensation temperature above the surface inversion layer. For temperatures prevailing over central Antarctica, resulting precipitation rates are typically halved for a surface cooling of 10°C. At the margin, the precipitation ratio is closer to 0.6 for an identical temperature shift.

4.1.3. Basal melting rate below the ice shelves

In Huybrechts and de Wolde (1999), the basal melting rate below the ice shelves was shown to exert a significant influence on the position of the grounding line, similar to the role of ice-shelf effective viscosity changes. Viscosity changes are treated similarly to Huybrechts and de Wolde (1999) by considering an effective ice-shelf deformation temperature that follows half of the applied surface-temperature change by a characteristic time lag of 500 yr. The basal melting rate S ($m\,yr^{-1}$), on the other hand, is non-zero for present conditions and forced to follow general climatic trends as follows:

$$\frac{dS}{dt} = -\frac{1}{\tau_s}(S - S_r),$$

$$S_r = S_0 b^{c\Delta T_{VA}}, \quad (4)$$

where S_r is the equilibrium melting rate for a climatic forcing equal to ΔT_{VA}, S_0 is the present basal melting rate and b and c are parameters which control the temperature sensitivity of S. For the reference experiment, $S_0 = 0.4\,m\,yr^{-1}$, $b = 1.2$ and $c = 1$. The value for S_0 corresponds to a total melt rate of about $540 \times 10^{12}\,kg\,yr^{-1}$ below the present ice shelves, or intermediate to the range of $320–756 \times 10^{12}\,kg\,yr^{-1}$ found in the literature (Kotlyakov et al., 1978; Jacobs et al., 1992, 1996). A clear relation between climatic change, oceanic circulation, oceanic temperature, and basal melt rates can however not be established from available oceanographic studies (Nicholls, 1997; Grosfeld and Gerdes, 1998; Williams et al., 1998). In our approach, it is therefore simply assumed that the basal melt rate is reduced by 20% for every degree of atmospheric temperature change, yielding a reduction to 15% of its current value for a typical glacial cooling of 10°C. The e-folding relaxation time $\tau_s = 100\,yr$ is introduced to account for the oceanic delay with respect

to atmospheric temperature changes, though its value is trivial in the context of glacial–interglacial changes. It is however realized that basal melting below the ice shelves is a much more complicated process than can be accounted for here, and depends on factors such as summer ocean warming, length of period with open water, thermohaline properties of the source water, and the details of the water circulation below the ice shelves. Nor is it reasonable to expect a uniform rate as both basal melt rates in excess of $10\,\mathrm{m\,yr^{-1}}$ and basal accretion rates are presently observed (Oerter et al., 1992; Jacobs et al., 1996), but our present understanding does not allow for a much more sophisticated treatment, especially for different climatic regimes and/or ice shelf geometries. The parameter values in Eq. (4) were chosen in order to produce reasonable results, but are tested in Section 4.4 further below.

4.1.4. Sea-level forcing

The sea-level forcing (Fig. 1, lower panel) constitutes an important control on grounding-line changes and was derived from the SPECMAP stack (Imbrie et al., 1984), using a conversion factor of –34.83 m of sea-level per ‰ of the marine oxygen-isotope values. This record slightly lags the Vostok record for the last two glacial cycles as might be expected, but precedes the temperature forcing by several thousand years before that. However, no phase shifts were applied to the forcing functions to alleviate the dating inconsistency for the first two glacial periods. The maximum sea-level depression is 130 m at 19 kyr BP (calendar years).

4.2. Results of the reference experiment

Fig. 2 displays the modelled evolution of grounded ice volume and ice-sheet area over the last 405 kyr. These are calendar years as defined by the chronology of the forcing. It can be seen that for much of the simulation, the Antarctic ice sheet fluctuated around an intermediate position, with only two glacial–interglacial transitions resembling the last one. The total volume range over the period is about $11.3\times10^{6}\,\mathrm{km^3}$. This corresponds to a sea-level change of about 23 m, but the relation with ice volume is not linear as corrections have to be made for the effects of isostatic depression and for ice displacing ocean water. The exact timing of the LGM in Antarctica is difficult to establish unambiguously, but is shown to significantly lag the commonly employed date of 21 kyr BP. According to the model, the Antarctic ice sheet reached its maximum extent around 15 kyr BP, but remained close to this position for much of the time between 20 and 10 kyr BP. Maximum volume, on the other hand, is only reached around 10 kyr BP, after which Holocene retreat sets in (Fig. 2). This late retreat is a distinct feature of the model and an important difference with the situation on the northern hemisphere. The retreat takes about 6–8 kyr to complete to reach a minimum shortly after the present time, after which the grounding line advances again. The extension of the simulation into the future used a zero sea-level and temperature forcing.

4.2.1. Eemian minimum and glacial buildup

Fig. 3 shows snapshots of the Antarctic ice sheet at several stages during the last glacial cycle. The location of geographic names is shown in Fig. 4. The ice sheet during the Last Interglacial at 120 kyr BP (Eemian) is somewhat smaller than today, in particular in the Ronne-Filchner basin, where the grounding line has retreated to more inland positions by 50–150 km. The implied eustatic sea-level rise is 1.4 m. During the subsequent glacial buildup, a moderate lowering of global sea level by some 35–40 m is enough to initiate grounding in the Amery basin and the Weddell Sea, where the ice shelf runs aground on a number of sea-bed

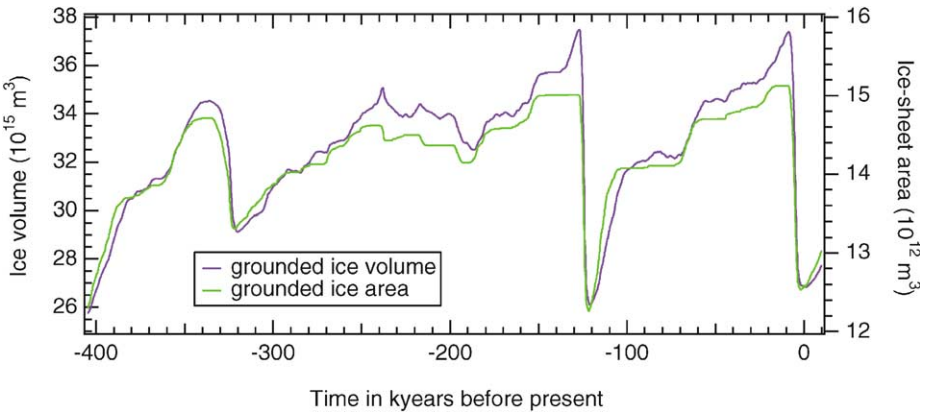

Fig. 2. Evolution of grounded ice volume and grounded ice-sheet area of the Antarctic ice sheet in the reference experiment (A0) over the last four glacial cycles.

highs close to the present ice shelf front (picture at 80 kyr BP). This obstructs the ice flow landinwards and causes a relatively rapid thickening by a back-filling mechanism, so that almost instantaneous grounding occurs over a large area. The situation in the Ross Sea, on the other hand, is quite different. Here, the free water depth below the ice shelf generally increases towards the sea and consequently, grounding is of a more gradual nature. Also the threshold for grounding appears to be larger and widespread grounding is only produced in the later stages of a glacial period, in particular when the global sea-level depression exceeds 100 m.

4.2.2. Last Glacial Maximum

By 15 kyr BP, the ice sheet reaches a maximum extent close to the continental break all around the continent. At this stage, the Antarctic ice sheet has grown to $37.7 \times 10^6\,\mathrm{km}^3$ at an area of $15.06 \times 10^6\,\mathrm{km}^2$, or increases of ca. 35% and 20% with respect to the present ice sheet, respectively. This corresponds to a sea-level lowering of 19.2 m with respect to the presently modelled ice sheet. Most of the ice-sheet advance is over the Weddell and Ross embayments, the Amery Basin, and around the Antarctic Peninsula. Around the East Antarctic perimeter, grounding-line advance is limited to 50–100 km at most in some places (Dronning Maud Land, Wilkes Land), but other parts of the coast had little or no advance of grounded ice. Surface elevation at the LGM was higher over most of the West Antarctic ice sheet and the Peninsula ice sheet by up to 2000 m, but lower over central East Antarctica by typically 50–100 m. This reflects the dominant influences of grounding-line advance and lower accumulation rates on the respective parts of the Antarctic ice sheet. Compared to the present ice sheet, the flow pattern and position of domes and ice divides of the East Antarctic ice sheet (EAIS) hardly changed during the LGM. By contrast, the model predicts significant changes of the flow direction elsewhere, particularly near the present grounding line of the Ross ice shelf, and in Palmer Land.

This result shares many of the features discussed in earlier work (Huybrechts, 1990, 1992), except that the total sea-level depression at the LGM predicted in this study is 4–5 m higher. That is because the current model predicts a further LGM extent of grounded ice in the Ross Sea, and because the baseline against which the comparison is made has less ice in the Antarctic Peninsula and the Amery Basin. The only other simulation of the Antarctic ice sheet to date with a comprehensive three-dimensional model is by Ritz et al. (2001). Their model is very similar to ours in many aspects but differs by the incorporation of a 'shelfy plate' between the grounded ice sheet and the floating ice shelf. Its occurrence depends on the magnitude of basal drag and is thought to represent a zone with ice streams. The result is a much flatter ice sheet at the LGM, in particular in the Ross Basin, and less extensive grounding elsewhere, yielding Antarctic LGM sea-level depressions that are only about half of those obtained in this paper.

4.2.3. Holocene retreat

The concomitant shrinking of the Antarctic ice sheet is essentially a partial disintegration of the West Antarctic ice sheet. Grounding-line retreat is triggered by a rise of world-wide sea level, but lags behind. In the model, it begins around 10 kyr BP to be nearly completed by the present time. The initiation coincides with a time of fast global sea-level rise (meltwater pulse MWP-1B) when about half of the total glacial/interglacial rise has already been completed (Fairbanks, 1989). There are two reasons for the delay with respect to the world-wide sea-level rise: first, the threshold for grounding-line retreat is usually higher than for grounding-line advance because the gradient of the height above buoyancy at the inland side is usually steeper than the gradient of the free water depth below the ice shelf at the seaward side; second, increased accumulation rates during the early stages of the Holocene thicken the ice and offset the retreating effect of rising sea level. The time lag between the onset of the recession and the beginning of the climatic warming is also the reason why the ice volume reaches a maximum during the early stages of the glacial–interglacial transition: at that time accumulation rates have already increased, while the ice-sheet domain has not yet started to shrink and the surface warming signal has not reached basal shear layers. In the reference run, the model predicts an additional sea-level lowering of 3.7 m between 21 and 10 kyr BP. Different thresholds for grounding-line migration also play for the retreat: in the model the Ross Basin ungrounds earlier than the Ronne-Filchner Basin. Similar variations of thresholds occur around the Antarctic Peninsula: ice-sheet retreat in Marguerite Bay and Alexander Island occurs several thousand years earlier than along the Lassiter and Orville Coasts (Fig. 3, lower row of pictures).

Another intriguing feature of the disintegration of the WAIS is that it seems to develop its own internally controlled dynamics: the environmental forcing stabilizes after 6 kyr BP, yet grounding-line retreat continues for thousands of years. It only stops when a new equilibrium can be established between sea depth and ice thickness, which occurs in the model during the next millenium. Apparently, the process of crustal rebound plays a crucial role as bed adjustments have a similar effect on grounding-line migration than global sea-level changes. Whereas surface elevations over the West Antarctic ice sheet continuously decrease during the Holocene, East Antarctic elevations mostly increase

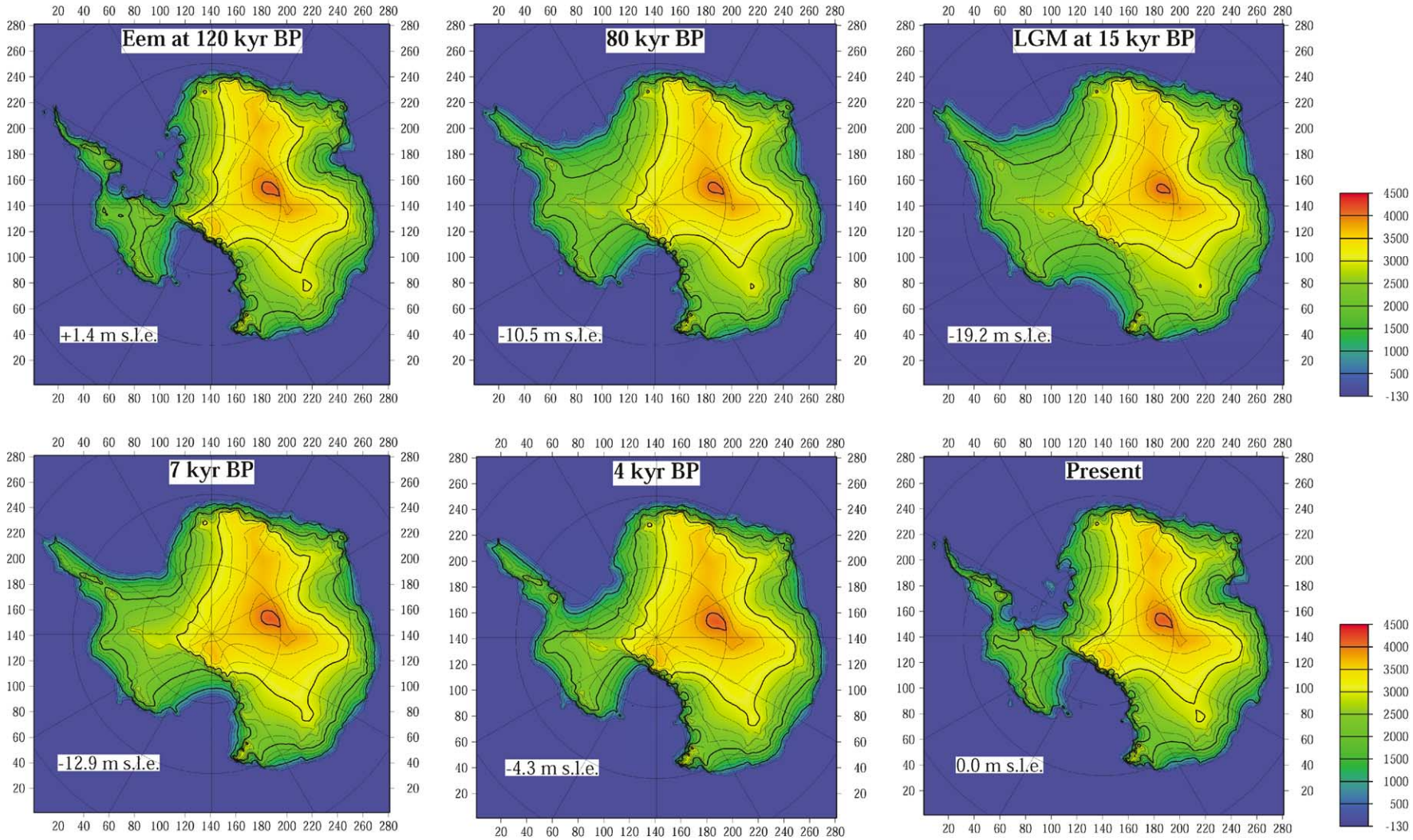

Fig. 3. Snapshots of Antarctica's ice-sheet evolution during the last glacial cycle in the reference experiment (A0). Shown is surface elevation relative to present sea level. Contour interval is 250 m; thick lines are for every 1000 m; the lowest contour is for 250 m and generally close to the grounding-line (s.l.e = sea-level equivalent).

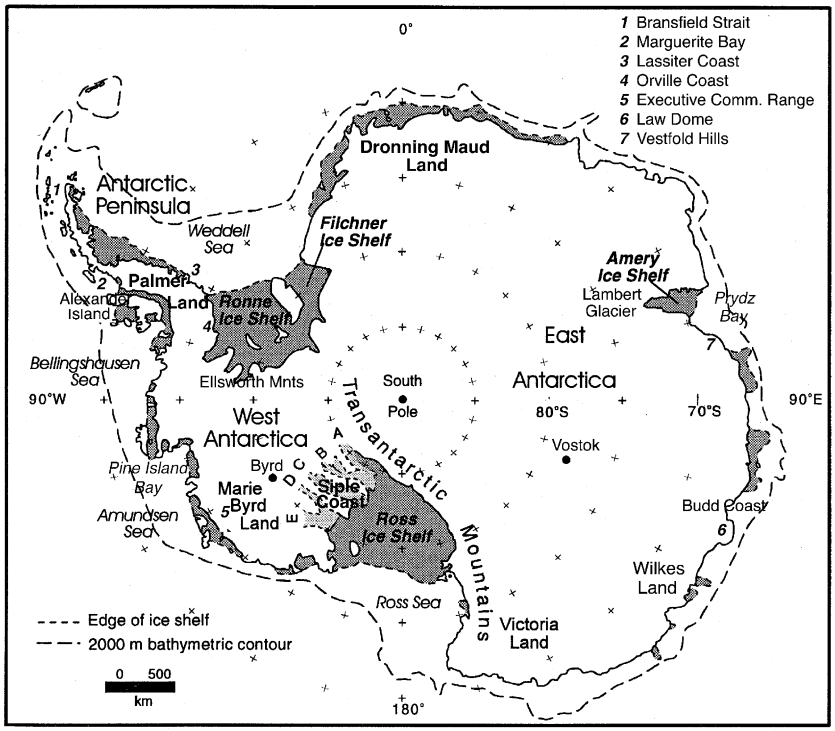

Fig. 4. Index map of Antarctic geographic locations mentioned in the text. Shaded areas are ice shelves.

after the LGM, though that a thinning wave caused by postglacial grounding-retreat and warming of basal layers progressively overturns the thickening from the coast inland.

The ice sheet simulated for the present-day (Fig. 3, lower right picture) is quite close to the observed one, especially over East Antarctica, but also the grounding line of the WAIS is reproduced in almost exactly the right place. This is an important validation of the model. Somewhat larger deviations from the observations, include the failure to resolve the narrow channel between Palmer Land and Alexander Island (George VI ice shelf), and the somewhat higher elevations of the WAIS of up to 250–500 m. The latter represents a systematic deviation with reality, but is taken into account in the results because differences are always taken between model states, and not between a model state and an observed state.

4.2.4. Loading and bedrock changes

Overall changes of the Antarctic ice sheet between the LGM and the present day are nicely summarized in Fig. 5. The geographical patterns of lithospheric loading changes and the associated glaciostatic uplift are shown. The integrated loading change (ice and water) within the grounded limit of the LGM ice sheet translates directly into global sea-level change; summing the loading and uplift patterns yields the corresponding elevation change for grounded ice and slightly underestimates the elevation change for the present ice shelf areas. The most pronounced features are linked to three main centres of unloading, respectively, situated over the Ross, Ronne Filchner, and Amery Basins, with maximum values in excess of 2.5 km of ice. The central plateau of the East Antarctic ice sheet, on the other hand, generally shows a thickening of up to 100–200 m in response to the increased accumulation rates, together with a fingerlike pattern of thinning that radiates inland from the main centres of outflow. Those are associated with grounding line retreat and increased outflow from both the East and West Antarctic ice sheets. Small thinning of less than 100–200 is simulated over the Executive Committee Range and in central Palmer Land. This unloading pattern is mirrored in the crustal uplift pattern (Fig. 5, lower panel). The effect is a much smoothed imprint because the lithosphere behaves as a low pass filter. Most of Antarctica exhibits an uplift with a maximum value of up to 600 m in the Ronne Filchner Basin, together with a pattern of crustal downwarping of less than 25 m in central East Antarctica and over the ocean. It is realized, however, that this pattern depends on the specific rheology employed, and that other solutions exist.

4.3. Comparison with field data

There are still many gaps in the glacial-geological record concerning the timing and the extent of the

Antarctic ice sheet at the LGM. Extensive reviews of the current evidence are presented in Bentley and Anderson (1998); Ingolfsson et al. (1998); Anderson (1999), and Bentley (1999). The broad picture emerging from these studies calls for an LGM expansion close to the edge of the continental platform, with a retreat lagging in time with respect to northern hemisphere melting that took at least 5000 yr to complete. This broad picture is well reproduced in the modelling, though one should keep in mind that the resolution of the model and other simplifications make that a detailed comparison at the scale of individual point observations should be reserved.

4.3.1. LGM extent and timing of Holocene retreat

One of the most contentious issues in older reconstructions concerned the LGM extent in the Ross Embayment, including the possibility of only a minor expansion in the inner Ross Embayment (Denton et al., 1989). Combined sedimentological and geophysical evidence reviewed in Anderson (1999) now strongly suggests that the LGM ice sheet was grounded near to the shelf break in the eastern Ross Sea but remained south of Coulman Island in the western Ross Sea, in close agreement with the model result for 15 kyr BP. This ice sheet was bordered by a grounding zone at least a few hundred km wide where major ice streams existed. Evidence on land indicates that the Holocene retreat reached Ross Island by 7 kyr BP (Ingolfsson et al., 1998) and that most of the remainder of the recession occurred at an approximately linear rate during the Middle and Late Holocene (Conway et al., 1999). Again, such a late retreat is well supported by the model. Conway et al. (1999) argue that grounding-line retreat could continue in the future, in which case complete deglaciation would take another 7000 yr to complete (Bindschadler, 1998). Here, however, the model offers a different view: whereas grounding-line retreat in the Ross Embayment is at present still occurring, recession is almost complete and is predicted to reverse in the second half of the next millenium. This process appears to be closely linked to the speed and extent of isostatic adjustment in the Ross Sea, which causes ongoing retreat over an isostatically depressed bed that is eventually halted and reversed by delayed isostatic uplift.

In the Ronne-Filchner Embayment, current evidence indicates widespread grounding down to the outer continental shelf at waterdepths of 1000–1200 in the eastern part and the Crary Trough (the offshore extension of the Thiel Trough). The extent along the southwestern Weddell Sea shelf, on the other hand, is poorly constrained (Elverhøi, 1981; Bentley and Anderson, 1998). Age control is limited and the possibility exists that the maximum was reached sometime earlier than the LGM. For this area, the model yields a grounding line down to the continental break all along with a retreat history that lags events in the Ross Sea. The latter feature cannot be compared to available evidence and remains one of the key features of the model that remains untested.

For the Antarctic Peninsula, Bentley and Anderson (1998) reconstruct a grounding line at least to the middle shelf in the Weddell Sea, whereas the model places the LGM grounding line further down to the –500 m contour at the shelf break. At the western side, there is good evidence for substantial seaward expansion close to or at the shelf break in the Bransfield Strait, Marguerite Bay and Pine Island Bay (Clapperton and Sugden, 1982; Anderson, 1999), quite similar to the behaviour reproduced by the model. Data on the timing indicate that the retreat began first in the northern Peninsula area by about 14–13 kyr BP but substantially later by 6 kyr BP further south. The model also reproduces this north-south gradient, but later in time.

Information summarized in Bentley (1999) and Anderson (1999) for East Antarctica yields a picture of ice-sheet advance by 100–150 km on the Wilkes Land continental shelf, but only by 8–15 km down to the –200 m isobath along the Budd Coast (Goodwin, 1993). Many other parts of coastal East Antarctica seem to have remained unaffected by this glacial episode and remained ice-free. Anderson (1999) cites evidence indicating that the LGM grounding-line at the head of the Lambert/Amery system in Prydz Bay also extended down to the continental shelf. Here, retreat started around 11.5 kyr BP with a Mid-Holocene readvance between 7 and 4 kyr BP. Elsewhere at the Windmill Islands around Law Dome, retreat occurred between 8 and 5 kyr BP (Goodwin, 1993). These general features are quite well simulated by the model, except that the retreat in the Amery Basin occurs only after 4 kyr BP.

4.3.2. Inland elevation changes

Observational control on elevation or thickness changes of the inland ice is weak and limited to dated moraines along the flanks of coastal mountain ranges and analysis of ice core data. Ackert et al. (1999) find evidence for a 50 m higher than present glacier stand around Mount Waesche in the Executive Committee Range. This value compares well with the value for the nearest gridpoint in Fig. 5, which has a thinning of 58 m between 16 kyr BP and today. In their paper, Ackert et al. (1999) go on to conclude that such a small thinning might have applied to all of the Ross Basin, and thus that the LGM WAIS would have contained much less ice than often assumed. Closer inspection of Fig. 5, on the other hand, clearly indicates that such a conclusion need not necessarily be the case and that a small elevation change over the Executive Committee Range can be compatible with a much larger thinning elsewhere

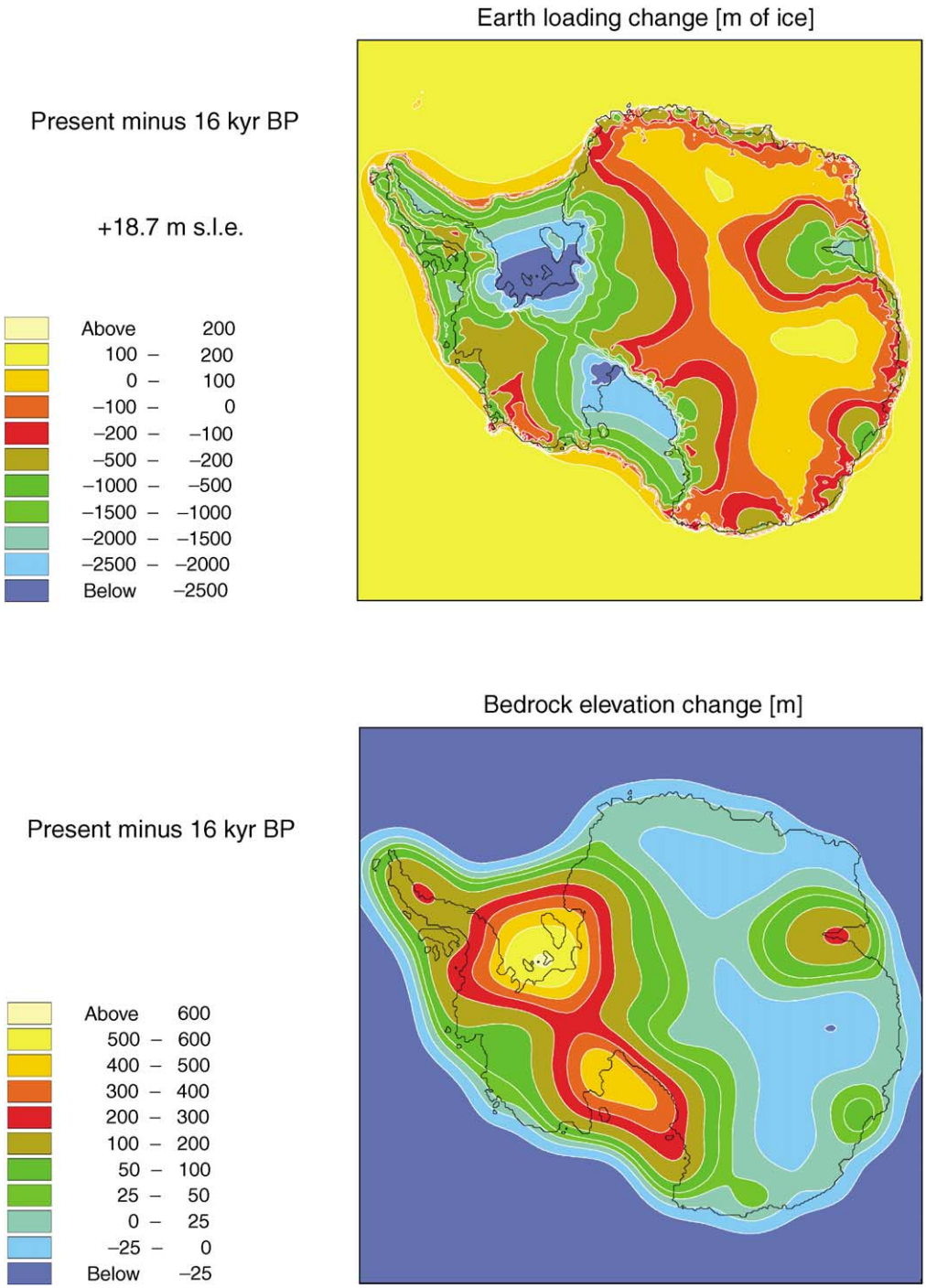

Fig. 5. Differences in Earth loading (upper panel) and bedrock elevation (lower panel) between 16 kyr BP and the present-day for the Antarctic reference experiment (A0). The Earth loading consists of both changes in ice loading and water loading, which are both expressed in (m) of equivalent ice load. Under the assumption of a constant oceanic area, the total loading change is equivalent to +18.7 m of global sea level. Bedrock elevation changes are relative to the present sea level. The background contour is the present grounding line of the initial data set, that is close to the modelled one for 0 kyr BP.

in West Antarctica. The reason is that the Executive Committee Range builds a separate dome which thickness changes are to a large extent decoupled form elevation changes elsewhere. Other data from nunataks in West Antarctic are also in good accord with the model, such as the inferred thinning of between 400 m (landward side) and 1900 m (seaward side) across the Ellsworth Mountains and of 500 m in Palmer Land (Bentley and Anderson, 1998), though the dating of moraine high stands is not firm.

Information based on ice cores, on the other hand, is conflicting. Byrd core $\delta^{18}O$ data imply that ice elevations were 500–600 m higher during the LGM (Jenssen, 1983; Grootes and Stuiver, 1986), but analysis of air content of the same ice core indicates thinner ice at the LGM and a thickening of 200–250 m between the end of the last ice age and the present day (Raynaud and Whillans, 1982, who attribute this to increased accumulation rates). The latter gas content results are however in dispute, and later work concludes that it is not clear how much of the gas changes are attributable to changes in atmospheric changes, and how much to elevation changes (Martinerie et al., 1994). The standard model run gives for Byrd Station an ice thinning of 760 m and a bedrock uplift of 175 m between 16 kyr BP and today. That implies an elevation decrease of 575 m, which is very close to the result derived by Jenssen (1983) from the $\delta^{18}O$ record. The corresponding numbers for Vostok station in East Antarctica are, respectively, 94, 18, and 76 m, but with a maximum elevation rise of 101 m at 4 kyr BP, decreasing since then (cf. Fig. 1). Observed estimates for ice thickening of between 600 m for Lambert Glacier and up to 1100 m over the Vestfold Hills are also in qualitative agreement with the data shown in Fig. 5.

4.3.3. Other reconstructions

A further comparison can be made with the LGM reconstruction of the CLIMAP-group (Denton and Hughes, 1981). Both our model and the CLIMAP reconstruction have in common that grounded ice expanded to the edge of the continental shelves in the Ross and Weddell Seas. The CLIMAP ice sheet was however substantially higher than our result with only one central dome located over East Antarctica, equivalent to a sea-level fall of between 24.7 and 29.2 m, depending on which rock-to-ice density ratio is preferred (Stuiver et al., 1981). By contrast, the glaciological model results presented in this paper clearly demonstrate that the respective ice domes are well preserved during a glacial cycle, and that the positions of ice divides, saddles, and local maxima show relatively small shifts, especially in East Antarctica. Also surface elevations over interior regions of East Antarctica (above the 2000–2500 contour) are predicted to have been lower during the LGM in accordance with the lower accumulation rates inferred from the Vostok ice core, whereas the CLIMAP reconstruction had a thicker East Antarctic ice sheet.

The agreement between CLIMAP and the LGM elevations of the WAIS in the model is generally better, at odds with a later reconstruction by Denton et al. (1986) that called for a low-lying WAIS with peripheral domes in the Ross and Weddell Seas. Lower elevations between 500 and 1000 m at the present grounding lines in the Ross and Weddell Seas (compared to the model result) are also preferred by Bentley and Anderson (1998). The surface profile of the West Antarctic ice sheet at the LGM represents a key difference between the model and most other post-CLIMAP reconstructions. That is because our model does not include a special treatment for individual ice streams or for ice resting on a soft bed, which could have played a role in case widespread ice stream flow comparable to the present Siple Coast continued to exist at the LGM. An upper bound on the possible overprediction of ice can be estimated by multiplying the present surface area of the WAIS and its continental shelf by an average ice thickness of 500 m and converting the result in sea-level equivalent. This yields $3 \times 10^{12}\,m^2 \times 500\,m \times 2.5 \times 10^{-15} = 3.7\,m$. Finally, additional support for a late Antarctic retreat is provided by glacio-isostatic studies (Tushingham and Peltier: retreat during 9–4 kyr BP; Peltier, 1994: 12–6 kyr BP; Nakada and Lambeck, 1988: 14–6 kyr BP), though their total LGM volumes equivalent to sea-level changes of between 22 and 37 m are much larger than deemed possible on glaciological grounds.

4.4. Sensitivity of the results

In order to test the robustness of the simulations, a series of sensitivity tests were set up in which crucial parameters were varied within their ranges of uncertainty. These experiments dealt with various aspects of internal dynamics (bedrock adjustment, basal sliding, thermomechanical coupling), the treatment of ice shelf response to climatic changes, and with the transfer functions between the Vostok deuterium record and prescribed temperature and mass-balance changes. Here we discuss only the results of those experiments that produced discernible changes of the Antarctic ice sheet. Table 1 gives an overview of the different model setups and parameter values. The corresponding results for 21 and 10 kyr BP are given in Table 2. The sea-level contributions relative to the reference run at present are displayed in Fig. 6 and the implied surface geometries for several minimum and maximum LGM (15 kyr BP) reconstructions are shown in Fig. 7.

4.4.1. The effect of internal dynamics

The curves displayed in the upper panel of Fig. 6 show how the overall dynamics of the (West) Antarctic ice sheet is sensitive to the speed of isostatic adjustment. The effect is most pronounced during glacial–interglacial transitions, when important ice-sheet changes take place over time periods comparable to the isostatic relaxation time τ_b. For the fast response case with $\tau_b = 1000\,yr$ (A1), the Earth's rebound causes grounding-line retreat to halt about halfway the present Ross and Weddell Basins, whereas the experiment with

$\tau_b = 10,000$ yr (A2) causes the ice sheet to retreat more inland by an opposite amount of equivalent sea-level change compared to the reference run A0 ($\tau_b = 3000$ yr). By contrast, the speed of rebound hardly influences ice-sheet behaviour during the much slower glacial build-up phase and at the LGM. This behaviour is similar to the runs discussed in Le Meur and Huybrechts (1996), and once more demonstrates the intricate relation between bed elevation, free water depth, and global sea-level changes during the retreat. If it is accepted that the ice-sheet model is basically correct, then the results seem to favour values for τ_b of at least 3000 yr. Doubling the basal sliding parameter (experiment A4) from 1.8×10^{-10} to 3.6×10^{-10} $N^{-3}\,yr^{-1}\,m^8$, on the other hand, does not distinguish between glacial buildup or glacial retreat, and merely offsets the evolution curve by a constant amount. That is because increased sliding enhances the flow, resulting in an overall ice-sheet thinning by 3–5% but this has little effect on the overall dynamic behaviour of the ice sheet.

4.4.2. The effect of the ice-shelf treatment

In previous work (Huybrechts and de Wolde, 1999), it was demonstrated how melting below the ice shelves and changes in effective viscosity crucially control ice shelf dynamics and grounding-line migration. That is because both affect ice-shelf thickness changes, that are eventually transmitted across the grounding-line and subsequently cause thickening/thinning of the grounding zone, and hence, grounding-line advance/retreat. Excluding thermomechanical coupling (experiment A3) does not allow for stiffer, and thus, thicker shelf ice

Table 1
Overview of model setup and forcing parameters for the experiments involving the Antarctic ice sheet

Exp. code	Description	Temperature forcing scaling (a in Eq. (1))	Temperature change for precipitation calculation (% of temperature forcing)	Ice shelf melting sensitivity (b/c in Eq. (4))	Ice shelf temperature change (% of temperature forcing)	Thermomechanical coupling	Isostatic relaxation time τ_b (yr)
A0	Reference	1	100	1.2/1	50	Yes	3000
A1	Fast bed adjustment	1	100	1.2/1	50	Yes	1000
A2	Slow bed adjustment	1	100	1.2/1	50	Yes	10,000
A3	Isothermal ice	1	100	1.2/1	0	No, ice at –8°C	3000
A4	High basal sliding	1	100	1.2/1	50	Yes	3000
A5	Constant ice shelf melting	1	100	1.0/0	50	Yes	3000
A6	High ice shelf melting sensitivity	1	100	1.4/1	50	Yes	3000
A7	High ΔT	1.5	67	1.2/0.67	33	Yes	3000
A8	High ΔT, high ΔP	1.5	100	1.2/1	33	Yes	3000
A9	High ΔT, ΔP, ice shelf ΔT	1.5	100	1.2/1	50	Yes	3000

Table 2
Grounded area and ice-sheet volume of the model runs involving the Antarctic ice sheet, together with the corresponding global sea-level contributions relative to the present modeled ice sheet in the reference experiment (volume = 27.92×10^6 km^3, area = 12.56×10^6 km^2)[a]

Exp.code	Description	Area at 21 kyr BP (10^6 km^2)	Volume at 21 kyr BP (10^6 km^3)	Sea level equivalent at 21 kyr BP (m)	Area at 10 kyr BP (10^6 km^2)	Volume at 10 kyr BP (10^6 km^3)	Sea level equivalent at 10 kyr BP (m)
A0	Reference	15.02	37.07	−17.57	15.06	38.61	−21.28
A1	Fast bed adjustment	14.99	37.02	−17.47	15.05	38.58	−21.22
A2	Slow bed adjustment	15.01	37.04	−17.50	15.07	38.55	−21.18
A3	Isothermal ice	13.68	30.55	−3.23	13.74	32.05	−6.85
A4	High basal sliding	15.07	35.74	−14.15	15.18	37.29	−17.78
A5	Constant ice shelf melting	14.22	33.91	−10.91	14.32	35.38	−14.42
A6	High ice shelf melting sensitivity	15.00	37.07	−17.58	15.06	38.59	−21.26
A7	High ΔT	14.92	37.59	−19.01	15.04	39.10	−22.64
A8	High ΔT, high ΔP	14.78	35.29	−13.44	14.95	37.52	−18.81
A9	High ΔT, ΔP, ice shelf ΔT	15.95	38.99	−20.72	15.85	40.66	−25.25

[a] Twenty-one kilo years BP is close to the commonly accepted date for the LGM, but the maximum area in most of the Antarctic runs is reached around 15 kyr BP, and the maximum volume is reached close to 10 kyr BP. Ice volumes are transformed into global sea-level changes taking into account the effects of isostatic depression and of ice replacing sea water, assuming an ice density of 910 kg m^{-3} and a constant oceanic surface area of 3.62×10^8 km^2, or 71% of the Earth's surface.

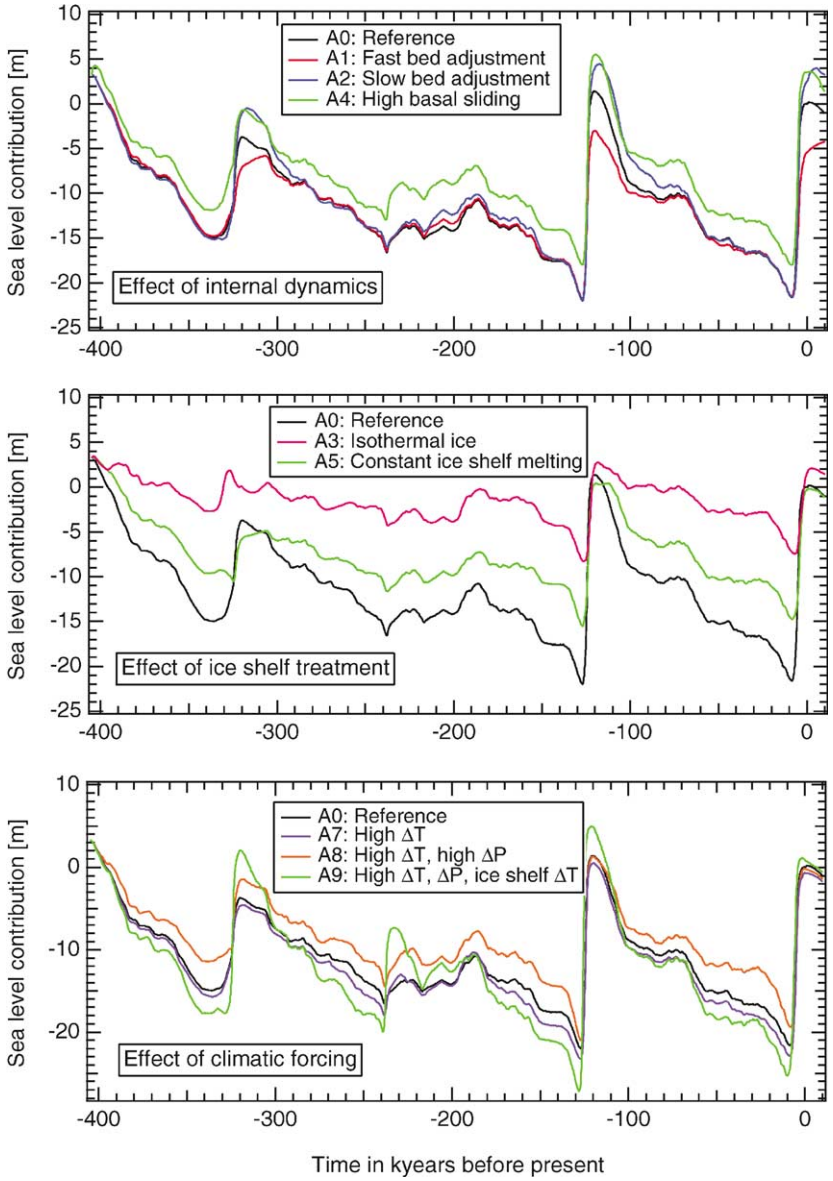

Fig. 6. Evolution of equivalent sea-level changes for the Antarctic reference experiment (A0) and a series of sensitivity experiments which test the effect of bedrock adjustment and basal sliding (upper panel), the effect of thermomechanical coupling and ice shelf melting (middle panel), and the effect of the mass balance and temperature forcing (lower panels). Experiment codes refer to the details of the model setup and parameter values given in Table 1.

during glacial periods, and therefore results in less grounding-line advance. A comparable effect is caused by keeping basal melting rates fixed at their present value of $0.4\,\mathrm{m\,yr^{-1}}$ (experiment A4, and Figs. 6 and 7). Both experiments affect grounding-line advance most in the Ross Basin, and much less elsewhere. Apparently, lower global sea levels are a necessary condition for grounding-line advance, but not sufficient, and additional processes in the ice shelves caused by temperature changes either weaken or strengthen the response. For experiment A3 (isothermal ice), the maximum sea-level depression at the LGM is only $\sim 7\,\mathrm{m}$, even less than the $\sim 14\,\mathrm{m}$ for experiment A5 (constant ice shelf melting). The latter is because the isothermal ice run also excludes the thickening of continental ice towards the end of a glacial period caused by a cooler base, as their LGM surface areas are much more similar. Increasing the temperature sensitivity of the basal melting rate from $20\%^{\circ}\mathrm{C}^{-1}$ to $40\%^{\circ}\mathrm{C}^{-1}$ (experiment A6), on the other hand, hardly makes a difference for the LGM ice sheet (Table 2).

4.4.3. *The effect of climatic forcing*

In the reference experiment, the transfer function between the Vostok deuterium record and temperature change assumed that today's spatial dependence

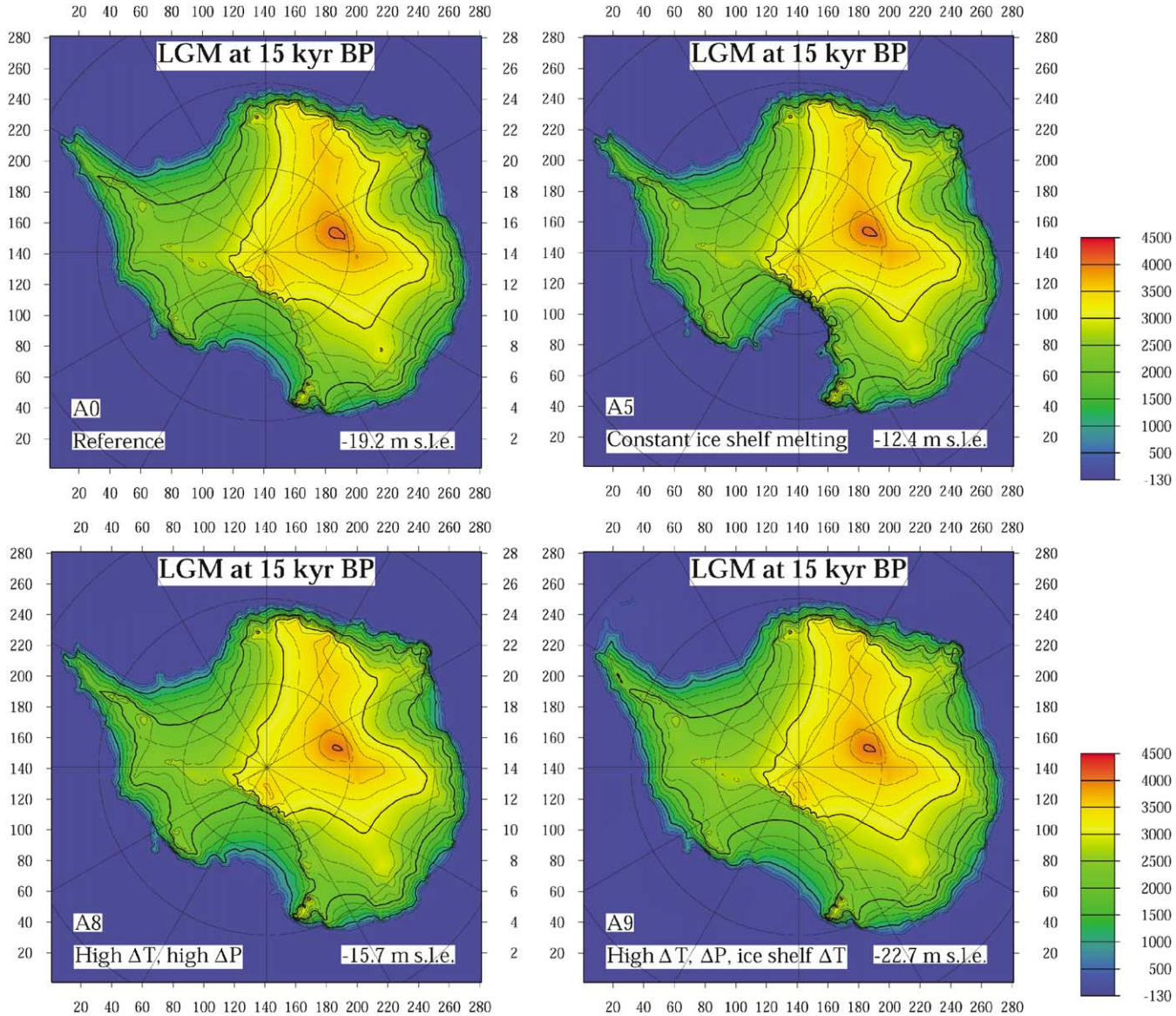

Fig. 7. Antarctic surface elevation at 15 kyr BP for the reference experiment and three sensitivity tests that produce significant changes of the ice-sheet geometry. Elevations are relative to current sea level. Contour interval is 250 m; thick lines are for every 1000 m; the lowest contour is for 250 m and generally close to the grounding line. The experiment codes refer to the details of the model setup provided in Table 1. (s.l.e = sea-level equivalent).

between isotope ratio and temperature can be transformed into temporal changes of the past (Petit et al., 1999). This procedure probably underestimates temperature changes by a factor 2 in Greenland (Johnsen et al., 1995), but is still widely accepted to hold true for Antarctica. However, interpretation of borehole temperatures at Vostok suggest that the true surface temperature change may have been underestimated by up to 50% (Salamatin et al., 1998), whereas other studies have even considered a factor two scenario for Byrd, West Antarctica (Blunier et al., 1998).

To account for this potential range, we therefore also ran a cold scenario by a factor 1.5 ($a = 1.5$ in Eq. (1)), with and without the concomitant additional lowering of the precipitation during cold periods (experiments A7 and A8). In both experiments, ice shelf viscosity changes were identical to the reference experiment but basal melting below the ice shelves followed the 1.5 times T-forcing for experiment A8. This is seen to produce an LGM ice sheet extent similar to the reference experiment (Fig. 7), but with a different surface elevation, especially over East Antarctica. Corresponding sea-level contributions at 15 kyr BP are only $\sim$15 m for the high

precipitation sensitivity case (A8), but ~21 m for the case in which precipitation amounts were roughly halved in accordance with a surface cooling of about 10°C (A7). Only if the ice shelf is allowed to stiffen additionally to reflect the higher temperature reduction (experiment A9), grounded ice expands far enough across the continental shelf to cause a sea-level depression of between 20 and 25 m for the duration of the LGM.

In all, however, it seems difficult to put more than ca. 20 m in the Antarctic ice sheet at the LGM, except when a significantly higher temperature reduction is applied which makes the ice cooler and stiffer, and hence, thicker. However, this is likely to be an extreme scenario as Vostok temperatures were probably not so low at the LGM, though changes elsewhere may have been larger (e.g. at Byrd).

5. Simulations of the Greenland ice sheet

5.1. Model forcing

The Greenland forcing is also driven by a background temperature change ΔT_{SG}, which is uniformly distributed over the ice sheet and throughout the year, and a prescribed sea-level record, from which the coastline is reconstructed that delimits the maximum extent of the ice sheet.

5.1.1. Temperature forcing

The temperature forcing is obtained from a synthetized $\delta^{18}O$ record representative for central Greenland conditions that spans the last two glacial cycles starting at 225 kyr BP. As in Cuffey and Marshall (2000), this isotope record is assembled from the GRIP $\delta^{18}O$ record (Dansgaard et al., 1993) for the most recent 100 kyr, and from the Vostok deuterium record (Petit et al., 1999) for the period prior to 100 kyr BP. The latter is scaled to the observed $\delta^{18}O$ amplitude of the GRIP record for the same time interval (Fig. 8). Reconstructing the climatic forcing for Greenland in this way seems a sensible thing to do because of the known defects of the GRIP δ record during the Eemian. The approach is justified by the generally good correlation of major climatic trends between the two hemispheres during the last 100,000 yr when the two ice core records are believed to be little disturbed, and enables to create a more credible forcing for the Greenland ice sheet during periods when the GRIP record is less reliable.

The fabricated isotope values for central Greenland are transformed in elevation-independent temperature changes according to

$$\Delta T_{SG}(t) = d(\delta^{18}O(t) + 34.83) - \Delta T_{SC}(t), \quad (5)$$

where d is a $\Delta T/\delta^{18}O$ conversion factor and ΔT_{SC} is a correction term for the change of altitude of the central dome during the ice sheet's evolution. It is equal to the summit elevation changes in the reference experiment, multiplied by the observed atmospheric lapse rate of −0.00792 (Huybrechts and de Wolde, 1999), cf. Fig. 8. The standard value for d is set at 2.4°C/‰. This is close to the intermediate values suggested by Lang et al. (1999) and Severinghaus and Brook (1999) on the basis of the isotopic ratio of atmospheric nitrogen and argon, but is allowed to vary in the experiments later to cover its full range suggested in the literature. Except during the Eemian and the Holocene, when elevation changes of the central dome are not predominantly driven by accumulation changes or when δ changes are small, the inclusion of ΔT_{SC} approximately increases the GRIP temperature forcing by 10%. d is viewed here as a constant and equal to the α_{obs}^{-1} as defined in Cuffey (2000), thus ignoring the additional effect of elevation changes on the climatic isotopic sensitivity that could potentially be important for small temperature changes like those of the Holocene. The approach adopted here also lacks the rigorous internal consistency of the theory developed in Cuffey (2000), which proposes a direct elevation correction on the $\delta^{18}O$ values rather than the separation in a climatic component and an elevation component as in Eq. (5). However, given the uncertainties on the vertical lapse rate and the elevational isotopic sensitivity, the outcome is very similar.

5.1.2. Precipitation forcing

As in previous studies with earlier versions of the model, the presently observed precipitation rate is taken as a base and prescribed to vary in proportion to the mean annual air temperature change on the ice sheet as follows:

$$P_G(x,y,t) = P_G(x,y,0)\exp\left[f\left(\delta^{18}O(t) + 34.83 + \frac{\Delta T_E(x,y,t) - \Delta T_{SC}(t)}{d}\right)\right], \quad (6)$$

where $P_G(0)$ and $P_G(t)$ are precipitation rates (m yr^{-1}) for present conditions and for a perturbed climate, respectively, f is an exponential factor, $\Delta T_E(x,y,t)$ is a spatially dependent temperature change resulting from local elevation changes anywhere on Greenland, and ΔT_{SC} was defined above. In the standard case, $\Delta T_E(x,y,t) = 0$ and $f = 0.169$. For $d = 2.4$°C/‰, this value of f corresponds to a 7.3% change of precipitation rate for every °C of temperature change. We prefer to link changes in the precipitation rate directly to the isotope values because that corresponds to the correlations made in the literature, and because different studies have used different temperature/isotope coefficients to transform the result in a temperature sensitivity

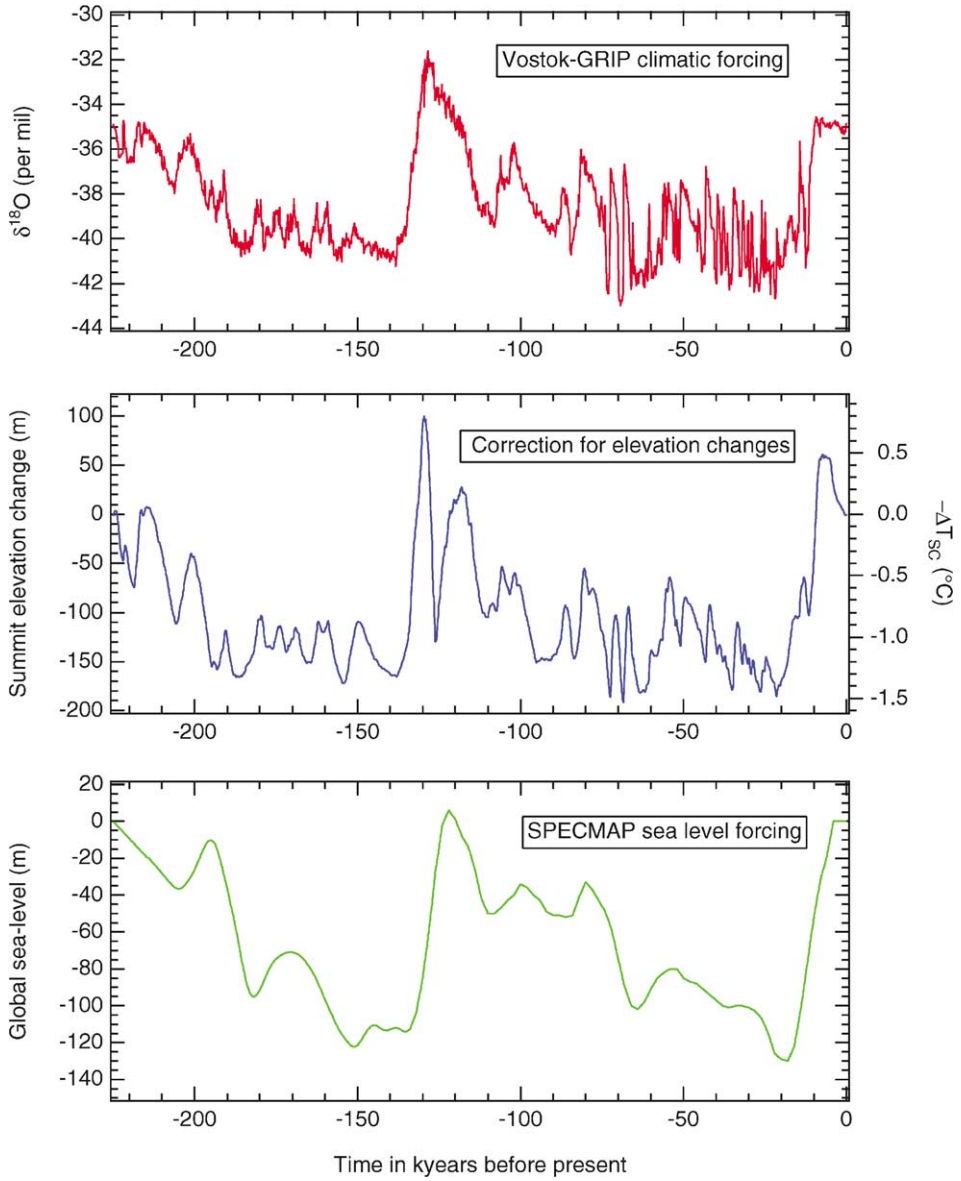

Fig. 8. Climatic (upper panel) and sea-level (lower panel) forcing used to reconstruct the history of the Greenland ice sheet over the last two glacial cycles. The δ record is synthetized from the Vostok deuterium record (for the period older than 100 kyr BP) and the GRIP oxygen-isotope record for the most recent 100 kyr, to circumvent known problems with Greenland records for the Eem, and should not be confused with a real existing Greenland isotope record. Also, shown is the term required to correct for elevation changes of the central dome, which is taken from the reference experiment (G0) during the same time period (middle panel).

(Dahl-Jensen et al., 1993; Dansgaard et al., 1993; Kapsner et al., 1995; Cuffey and Marshall, 2000). It also enables to study the effects of the temperature and precipitation sensitivity separately in the experiments described later. For the maximum glacial temperature cooling of about 19°C at 21 kyr BP in the reference experiment (corresponding to a $\delta^{18}O$ shift of 7.9‰), precipitation rates are reduced to about 25% of their modern value. We do not distinguish between different precipitation sensitivities for different time intervals as suggested by Kapsner et al. (1995), because the emphasis is on the glacial/interglacial contrast and because such refinements have only marginal influence on the overall ice volume evolution. The base map for precipitation was revised from Ohmura and Reeh (1991) by incorporating the results of shallow ice cores taken during recent oversnow traverses in north Greenland (Jung-Rothenhäusler, 1998).

5.1.3. Sea-level forcing

As for the Antarctic experiments, the sea-level forcing ΔH_{sl} (m) was also derived from the SPECMAP stack, and made to start off with a zero sea-level change at 225 kyr BP. Between 4 kyr BP and the present time, ΔH_{sl}

was set to zero (Fig. 8). ΔH_{sl} is then transformed in a bathymetric forcing ΔH_c as follows:

$$\Delta H_c = 2\Delta H_{sl} \quad \text{for } \Delta H_{sl} > -80\,\text{m},$$

$$\Delta H_c = 2\Delta H_{sl} - 0.25(\Delta H_{sl} + 80)^2 \quad \text{for } \Delta H_{sl} < -80\,\text{m}. \tag{7}$$

The actual coastline is then made to coincide with the bedrock contour given by ΔH_c insofar it lies within the limits provided by the current coastline and a maximum glacial extent digitized from glacial-geological reconstructions (Funder, 1989; Funder et al., 1998). This approach is admittedly of a phenomenological nature, and is based on the assumption that grounded ice is able to advance over deeper water the colder the climate, and thus the lower the sea-level depression is. The parameters in Eq. (7) were chosen to roughly mimic the timing and extent of the advancing ice sheet over the continental shelf as evident from the sparse marine geological studies.

5.2. Results of the reference experiment

In earlier work, it was demonstrated that the present type of shear-stress driven continuity models is generally able to reproduce main features of the Greenland ice sheet quite well (Letréguilly et al., 1991b; Weis et al., 1996; Greve, 1997; van de Wal, 1999; Marshall and Cuffey, 2000). The evolution of the ice sheet during the last two glacial cycles is illustrated in Figs. 9 and 10. Fig. 11 shows an index map of Greenland with the location of geographic names.

5.2.1. Eemian minimum

The most conspicious feature over this period concerns the fate of the ice sheet during the Eemian interglacial, when temperatures in the reference experiment peaked up to 7°C higher than today and were more than 5°C warmer for a duration of almost 3000 yr. This resulted in massive marginal melting that caused the modelled ice sheet to shrink to a central-northern dome that existed together with small pockets of residual mountain glaciation over the southeastern highlands (Fig. 10). The remaining central ice cap covered less than half of the present ice-sheet in area and had only a third of its volume, or equivalent to a sea-level rise of about 5.5 m. It also had a much steeper slope related to the higher balance gradients, but the elevation and position of the summit dome was rather well conserved. Interestingly, the Eemian minimum at 123 kyr BP occurred almost at the same time as the SPECMAP sea-level maximum of 6 m at 122 kyr BP, and the results suggest that it may largely have been responsible for it.

5.2.2. The last glacial cycle

The Greenland ice sheet subsequently needed about 20,000 yr to build up to a state comparable to the present one and by 90 kyr BP it had occupied all available landspace and extended to the coast almost everywhere. Further growth of the ice sheet was by a slow advance over the continental shelf and by a gradual thickening caused by a slow cooling of basal deformation layers that made the ice stiffer. For most of the glacial period, the main wastage mechanism was calving of icebergs, except during the warm peaks of the recurring Dansgaard–Oeschger events that periodically resulted in runoff pulses. Major expansion on the middle and outer shelves, especially in the southeast, only occurred towards the end of the glacial period after about 30 kyr BP. According to the model, the maximum volume was reached at 16.5 kyr BP, but the ice sheet remained close to its maximum extent between 25 and 15 kyr BP. The maximum sea-level depression caused by the Greenland ice sheet is calculated to have been 3.1 m for the standard set of model parameters, corresponding to a total ice volume of 4.4 million km^3, or 40% higher than today (Table 4). Note that the sea-level value is not corrected for ice displacing ocean water and for isostatic

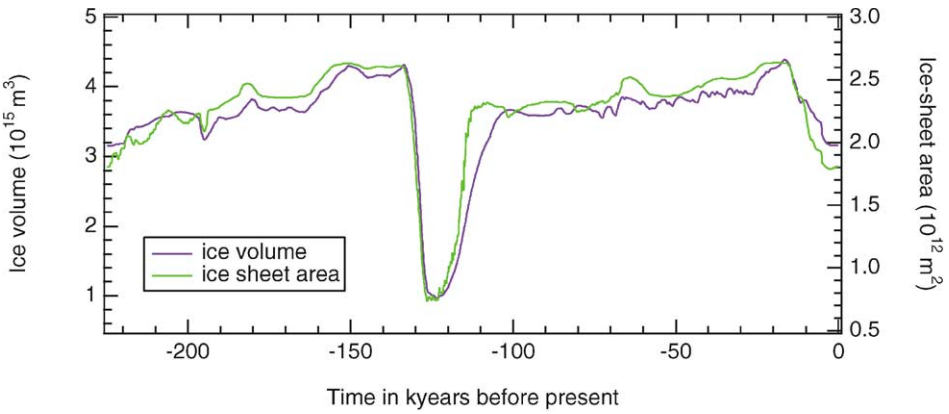

Fig. 9. Evolution of ice volume and ice-sheet area of the Greenland ice sheet in the reference experiment (G0) over the last two glacial cycles.

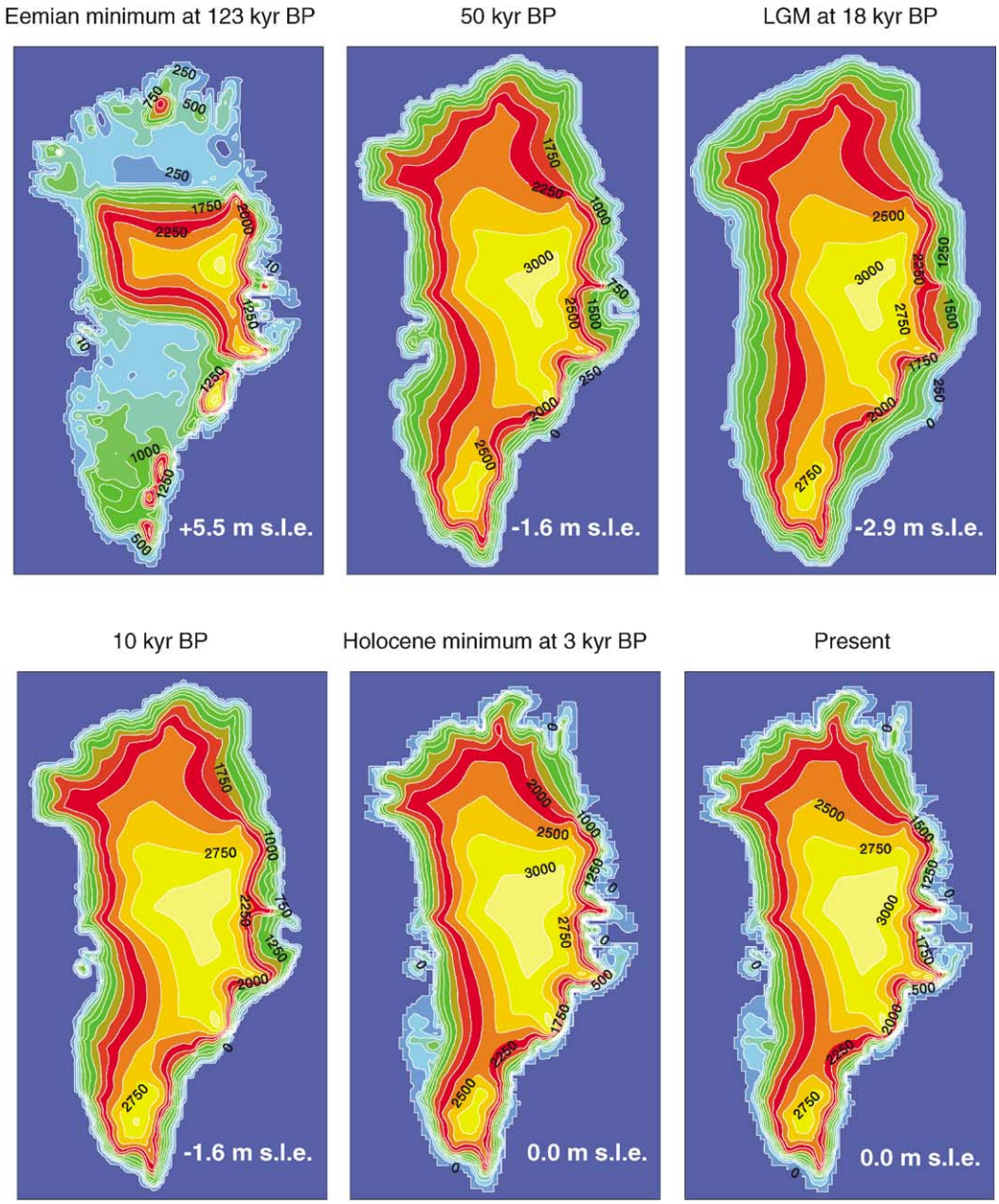

Fig. 10. Snapshots of Greenland's ice-sheet evolution during the last glacial cycle in the reference experiment (G0). Surface elevations are shown relative to present sea level. The ice-sheet margin is distinguished by its high surface slope and close contour-line spacing. Contour interval is 250 m. The numbers in the lower right corner are for equivalent sea-level change.

adjustment beyond the current coastline, but these effects are minor for Greenland.

By 10 kyr BP, the Greenland ice sheet had retreated to a position close to the present coastline (Fig. 10). At that stage, melting took over as the main mechanism of mass loss and further retreat occurred over land, thereby creating a coastal tundra belt, especially in the southwest. Retreat was virtually complete by 4.5 kyr BP. The model predicts a minimum state in the southwest at about 3 kyr BP, when the margin retreated to a more inland position than today by up to 50 km. In the last plot of Fig. 10, it is demonstrated that the model is able to reproduce an ice sheet that closely resembles the presently observed one.

Compared to most previous glacial cycle simulations of the Greenland ice sheet, the amplitude of the volume response is found to be much larger, with both a much reduced ice sheet during the Eemian and a more expanded ice sheet at the LGM. This is largely due to the adopted new temperature-isotope calibration as suggested by recent work (Cuffey, 2000), and to a lesser extent to a larger seaward expansion on the continental

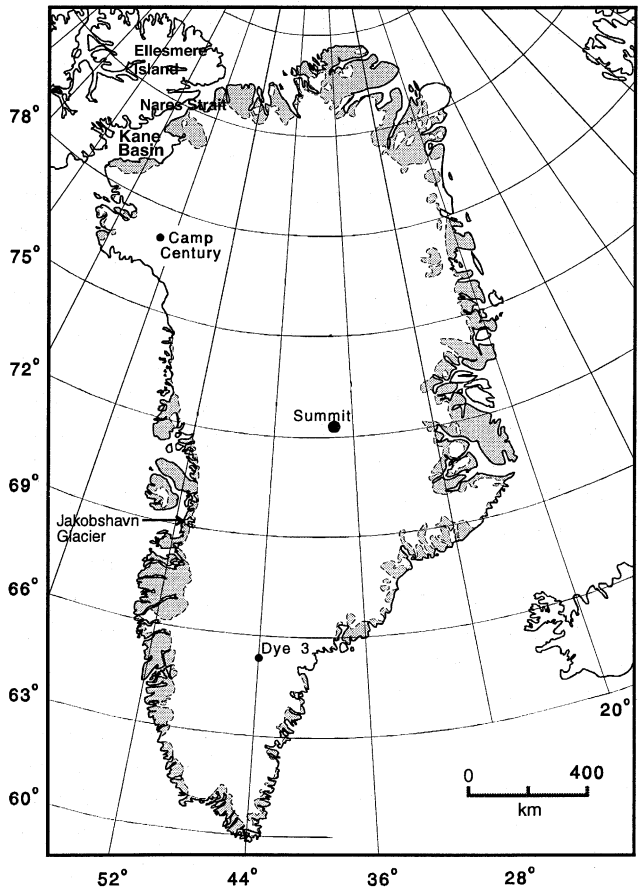

Fig. 11. Index map of geographic locations in Greenland mentioned in the text. Shaded areas represent ice-free land.

shelf. The result is quite similar to the recent reconstructions by Cuffey and Marshall (2000) and Marshall and Cuffey (2000). The timing of the LGM and Holocene retreat, on the other hand, is not much different from older simulations, as the chronology is mainly set by the environmental forcing.

5.2.3. Loading and bedrock changes

Loading changes between the LGM at 18 kyr BP and the present day show a pattern of central thickening of up to 200 m and a peripheral belt of thinning of 1–1.5 km around the margin, which is well reflected in the corresponding uplift pattern (Fig. 12). The thickening of the central dome occurs despite a shrinking of the total area and is due to the lower accumulation rates during glacial times, similar to the situation in East Antarctica. Although the isostasy models are not identical and rheologies differ, a comparison with the results published in Le Meur and Huybrechts (1998) shows that the patterns are very similar, but that the magnitudes of the ice thickness and bedrock changes are somewhat larger by up to a factor 2 because of the larger amplitude of the volume response. It should be noted that the glaciostatic response pattern excluded the effects of loading changes over the nearby American continent, which may have influenced west Greenland, but took into account the effect of the changing water loading over the ocean.

5.3. Comparison with field data

Observational evidence on the past size and extent of the Greenland ice sheet is almost solely restricted to marine evidence of its LGM position on the continental shelf and to a chronology of Holocene retreat on land, cf. reviews by Kelly (1985), Weidick (1985), Funder (1989), Funder et al. (1998), and Solheim et al. (1998).

5.3.1. LGM extent

As a broad picture, available data indicate that at the LGM virtually all of the Greenland continent was covered by ice which extended over at least the inner shelf. This maximum was probably preceded by an even larger maximum during the Saalian around 150 kyr BP. Comparison of the observed LGM extent with the simulated extent is however not a very strong test of the model, because the maximum extent was already prescribed beforehand as a glaciation limit in case the surface mass balance allowed for it. According to Funder (1989) and Funder et al. (1998), glaciers at the LGM filled fjord basins and the inner shelf over a distance of only a few tens of km offshore in east and northeast Greenland, but between 30 and 60 km in west Greenland and up to a maximum of 200 km in the southeast. In the latter sector, marine evidence indicates that the ice extended furthest in the transverse shelf troughs downstream the major overdeepened outlet glaciers (Solheim et al., 1998). This maximum occurred between at least 22 and 14 kyr BP.

5.3.2. Holocene retreat

Disintegration of marine parts was underway by 13–12 kyr BP in the south, but occurred significantly later between 10 and 8 kyr BP in the north and northeast, in good agreement with the model results. The chronology of Holocene retreat is best documented in west Greenland (Kelly, 1985; Weidick, 1985), where periods of recession are interrupted by periods of relative standstills that left a succession of datable strandlines and moraines. The ice sheet retreated to approximately the present coastline by 10 kyr BP and melted further back inland to near its present position by about 6 kyr BP. In central west Greenland, the ice sheet eventually retreated to a position at least 15 km behind its present position between 6 and 3 kyr BP, as documented by the presence of reworked early Holocene marine biogenic material and shells (Weidick et al., 1990). In the northwest, the ice sheet never melted back from the sea-fronting position it occupied since 9–8 kyr BP. All of these features are very well reproduced by the

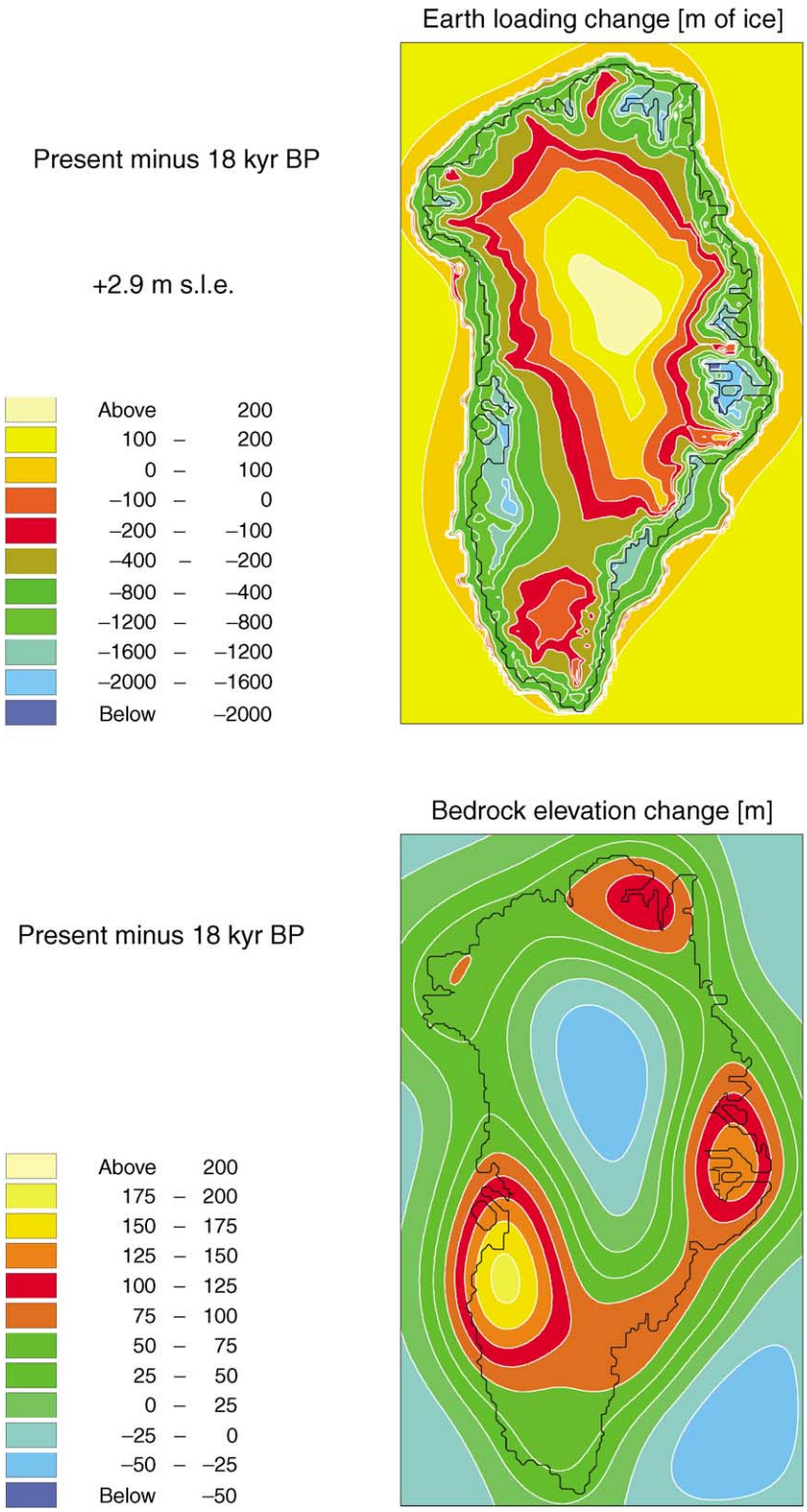

Fig. 12. Earth loading (upper panel) and bedrock elevation (lower panel) changes between 18 kyr BP and the present-day for the Greenland reference experiment (G0). The Earth loading consists of both changes in ice loading and water loading, which are both expressed in (m) of equivalent ice load. Under the assumption of a constant oceanic area, the total loading change is equivalent to +2.9 m of global sea level. Bedrock elevation changes are relative to current sea level. The background contour is the current coastline of the initial data set.

model, including the minimum inland position in the southwest by up to 50 km behind the present margin at 3 kyr BP. Van Tatenhove et al. (1995) made a careful comparison of available geological and glaciological (palaeo-) field evidence with the results of an earlier simulation that had a similar retreat history on land (Huybrechts, 1994). They found that the modelled retreat agreed to within 500–1000 yr of the glacial-geological reconstructions, or about the uncertainty on the ^{14}C ages of the dated moraines, along a transect parallel to 67°N extending from the present ice margin down to the continental shelf break. The Neoglacial advance culminated with the Little Ice Age 100–300 years ago, as predicted by the model. A similarly detailed chronology of Holocene retreat elsewhere in Greenland is however lacking.

5.3.3. Nares Strait

For a long time the possible coalescence of the Greenland and Canadian Arctic ice sheet to block Nares Strait was a subject of considerable debate. Denton and Hughes (1981) therefore presented two alternative reconstructions, one showing no connection with Ellesmere Island and another one showing Nares Strait entirely occupied by a transverse ridge 2500–3000 m high that connected the Greenland and Innuitian ice sheets and considerably changed ice flow patterns at both sides. This issue seems to be resolved in recent work (England, 1999; Zreda et al., 1999) which favours an intermediate solution in which Nares Strait was covered by a much thinner saddle during the LGM only (23–10 kyr BP). This saddle was centred over Kane Basin with the ice flowing north and south along the axis of Nares Strait and caused only little change of flow patterns on the Greenland ice sheet. In the modelling, the coalescence of both ice sheets was not considered and the maximum extent of the Greenland ice sheet was limited to the central axis of Nares Strait at an elevation at sea level. This probably ignores the additional ice which may have been contained in the Nares Strait within a sector roughly 500 km long, maximally 100 km wide, and perhaps on average 1000 m thick. That is equivalent to about 0.1 m of global sea level, small compared to the maximum Greenland sea-level depression of 3.1 m in the reference experiment.

5.3.4. Inland elevation changes

Information on elevation changes of the Greenland ice sheet is very limited. Jenssen (1983) estimated a lowering of about 1250 m at Camp Century between the LGM and 2.5 kyr ago, followed by a thickening of 400 m up to the present. This result was obtained from analysis of the total gas and stable isotope content, but this method to infer elevation changes has been severely questioned. The model, on the other hand, predicts for Camp Century an elevation increase of 100 m between 21 and 10 kyr BP, followed by a surface lowering of 70 m up to today. This reflects the effects of increased accumulation for the period prior to 10 kyr BP, when the margin remained approximately stationary, followed by the combined effects of a retreating margin and a basal warming of 2–3°C. Little evidence of significant elevation changes over the last two glacial cycles is also provided by central Greenland isotope records, and is corroborated by the model (Fig. 8). The model results are also in accord with the existence of pre-Eemian ice for the GRIP and GISP central Greenland Summit locations. This also applies to the assumed absence of pre-Eemian ice for the ice-core locations of Camp Century and Dye3, where the ice sheet was found to have disappeared between 126–123 kyr BP and 128–120 kyr BP, respectively. These results are supported by problems with the interpretation of the basal ice in these locations, which indicates no ice older than the last ice age (Koerner, 1989).

5.3.5. CLIMAP reconstruction

The model result for the LGM differs substantially from either the minimum or maximum CLIMAP reconstruction published two decades ago (Denton and Hughes, 1981), and which, respectively, contained 0.7 and 6.4 m of additional sea-level equivalent. The largest discrepancies concern the conservation of individual domes and the lower central ice-sheet elevations for the model because of the lower accumulation rates. The ice expansion, on the other hand, is generally close to the CLIMAP minimum for the northern half of the Greenland ice sheet, but closer to the CLIMAP maximum for the southern half.

5.4. Sensitivity of the results

The series of sensitivity tests mainly focused on the mass-balance treatment and the role of bedrock adjustment. The various model setups are detailed in Table 3. Table 4 gives results for 21 kyr BP and the Greenland glacial maximum at 16.5 kyr BP. The corresponding sea-level curves over the last two glacial cycles are displayed in Fig. 13 and the implied surface geometries for several LGM reconstructions are shown in Fig. 14.

5.4.1. The effect of internal dynamics

The speed of bedrock adjustment is tested in the experiments G1 and G2 (Fig. 13, upper panel). It can be seen that there is little effect from bedrock dynamics except during periods of rapid change such as during the Eemian, when large loading changes take place on time scales comparable to the isostatic relaxation time τ_b. The smallest Eemian ice sheet is associated with the longest isostatic response time. This is easily understood in terms of the elevation of the marginal melting zone

Table 3
Overview of model setup and forcing parameters for the experiments involving the Greenland ice sheet[a]

Exp. code	Description	d in Eq. (5) (°C/‰)	f in Eq. (6)	Precipitation sensitivity (%/°C)	Thermomechanical coupling	Isostatic relaxation time τ_b (yr)	ΔT_E in Eq. (6) (°C)
G0	Reference	2.4	0.169	7.3	Yes	3000	0
G1	Fast bed adjustment	2.4	0.169	7.3	Yes	1000	0
G2	Slow bed adjustment	2.4	0.169	7.3	Yes	10,000	0
G3	Isothermal ice	2.4	0.169	7.3	No, ice at –8°C	3000	0
G4	Precipitation change depends on elevation change	2.4	0.169	7.3	Yes	3000	From G0
G5	Low ΔT, mid ΔP	1.5	0.169	11.9	Yes	3000	0
G6	High ΔT, mid ΔP	3.0	0.169	5.8	Yes	3000	0
G7	Mid ΔT, low ΔP	2.4	0.115	4.9	Yes	3000	0
G8	Mid ΔT, high ΔP	2.4	0.225	9.8	Yes	3000	0
G9	Low ΔT, low ΔP	1.5	0.106	7.3	Yes	3000	0
G10	High ΔT, high ΔP	3.0	0.211	7.3	Yes	3000	0

[a] The parameter d is the temperature/isotope sensitivity, f controls the exponential dependence of precipitation changes on temperature or isotope changes, and ΔT_E is the local elevation change contributing to the local precipitation.

Table 4
Ice-sheet area and volume of the model runs involving the Greenland ice sheet, together with the corresponding global sea-level contributions relative to the present modeled ice sheet in the reference experiment (volume = 3.16×10^6 km^3, area = 1.80×10^6 km^2)[a]

Exp. Code	Description	Area at 21 kyr BP (10^6 km^2)	Volume at 21 kyr BP (10^6 km^3)	Sea level equivalent at 21 kyr BP (m)	Area at 16.5 kyr BP (10^6 km^2)	Volume at 16.5 kyr BP (10^6 km^3)	Sea level equivalent at 16.5 kyr BP (m)
G0	Reference	2.63	4.24	−2.72	2.63	4.39	−3.10
G1	Fast bed adjustment	2.63	4.23	−2.70	2.63	4.39	−3.08
G2	Slow bed adjustment	2.63	4.25	−2.75	2.63	4.40	−3.12
G3	Isothermal ice	2.63	4.11	−2.38	2.63	4.26	−2.76
G4	Precipitation change depends on elevation change	2.63	4.15	−2.49	2.63	4.29	−2.83
G5	Low ΔT, mid ΔP	2.63	3.93	−1.92	2.62	4.05	−2.25
G6	High ΔT, mid ΔP	2.63	4.44	−3.23	2.63	4.61	−3.63
G7	Mid ΔT, low ΔP	2.63	4.55	−3.50	2.63	4.68	−3.81
G8	Mid ΔT, high ΔP	2.63	3.96	−2.01	2.63	4.13	−2.45
G9	Low ΔT, low ΔP	2.63	4.29	−2.85	2.63	4.41	−3.13
G10	High ΔT, high ΔP	2.63	4.23	−2.68	2.63	4.41	−3.13

[a] Twenty-one kilo years BP is close to the commonly accepted date for the LGM, but the maximum area and volume in most of the Greenland runs is reached around 16.5 kyr BP. Ice volumes are transformed into global sea-level changes assuming an ice density of 910 kg m^{-3} and a constant oceanic surface area of 3.62×10^8 km^2, or 71% of the Earth's surface.

retreating over an isostatically depressed inland area. A faster rebound causes the ablation zone to uplift quicker to a higher, and hence, cooler, climatic regime which reduces melting. The value of τ_b makes hardly a difference for the size of the Greenland ice sheet at the LGM because the long build-up phase causes the ice sheet to be approximately in balance with the underlying lithosphere.

5.4.2. The effect of the temperature forcing

In the experiments, the temperature-isotope coefficient d (Eq. (5)) is allowed to vary between 1.5, the classical value derived from the spatial covariation of modern δ and T (Johnsen et al., 1989), and widely used in earlier modelling studies, and a value of 3, equal to double the spatial gradient as supported by borehole palaeothermometry (Johnsen et al., 1995; Cuffey and Clow, 1997; Dahl-Jensen et al., 1998). Under identical precipitation changes (experiments G5 and G6), this has the most severe consequences for the ice sheet during the Eemian. For the high temperature case (G6), Eemian temperatures peak at almost 10°C higher than today, and the ice sheet almost entirely disintegrates. Such a disintegration is however in conflict with the existence of

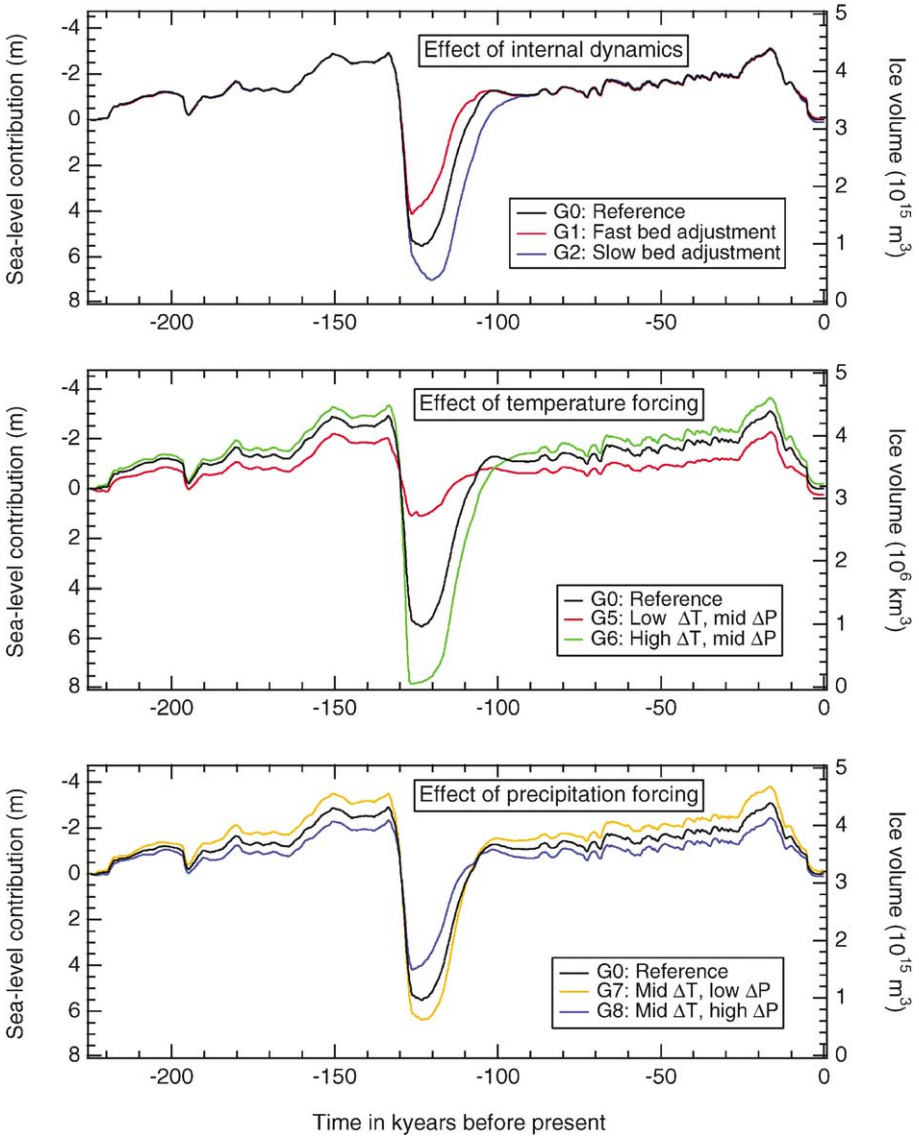

Fig. 13. Evolution of equivalent sea-level changes for the Greenland reference experiment (G0) and a series of sensitivity experiments which test the effect of bedrock adjustment (upper panel), the effect of the temperature forcing (middle panel), and the effect of the precipitation forcing (lower panels). Experiment codes refer to the details of the model setup and parameter values given in Table 3.

pre-Eemian ice in the GRIP record itself. Therefore, if it is accepted that the model is otherwise basically correct, this also suggests that the intermediate value of $d = 2.4$ (Lang et al., 1999) may be the more appropriate one. At the LGM, the investigated range in d only leads to a $\pm 5\%$ change in ice volume. This volume difference is only little influenced by differences of melting because ablation is insignificant for all three cases, but reflects the effects of thermomechanical coupling. For the high sensitivity experiment (G6), basal cooling is larger towards the end of a glacial period, leading to harder and thus thicker ice. This does not affect the overall surface morphology at the LGM, but mainly scales ice thickness by a constant fraction as shown in Fig. 14.

5.4.3. The effect of the precipitation forcing

The effect of varying the precipitation sensitivity for the full literature range of between $\sim 5\%\,^{\circ}C^{-1}$ (Clausen et al., 1988) and $\sim 10\%\,^{\circ}C^{-1}$ (Kapsner et al., 1995) is found to be of similar magnitude than the effect of the temperature-isotope sensitivity during the glacial period (Fig. 13, lower panel), but has less effect for the Eemian. A higher precipitation sensitivity leads to more precipitation during warmer periods and less precipitation during colder periods, and consequently a lower volume during the LGM and a higher volume during the Eemian as compared to the reference experiment. Introducing the additional temperature change arising from elevation changes to calculate precipitation changes as done in e.g. Letréguilly et al. (1991a,b), does

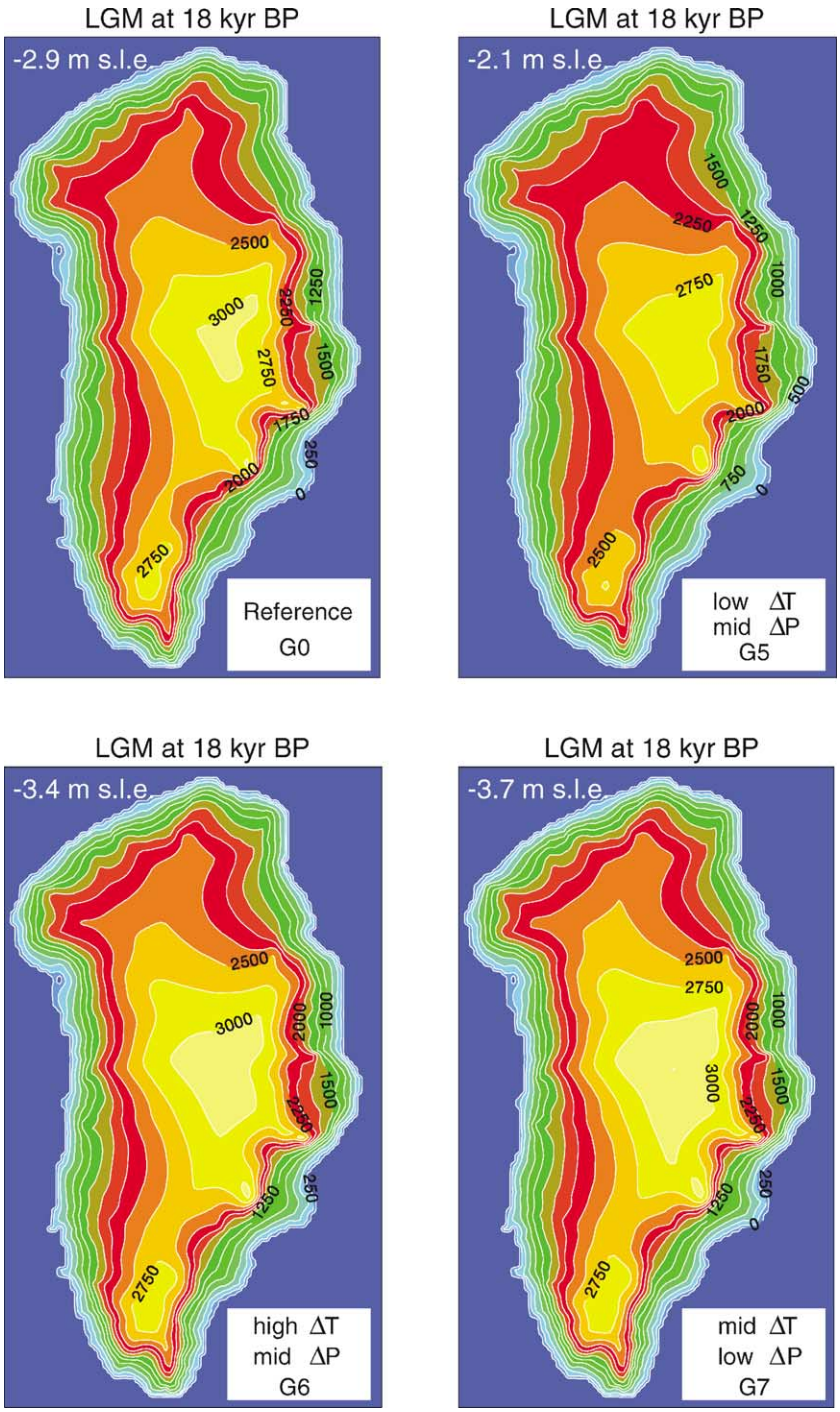

Fig. 14. Greenland surface elevation at 18 kyr BP for the reference experiment and three sensitivity tests that produce significant changes of the ice-sheet geometry. Elevations are relative to present-day sea level. The ice-sheet margin is distinguished by its high surface slope and close contour-line spacing. Contour interval is 250 m. The experiment codes refer to the details of the model setup provided in Table 3. The corresponding contributions to global sea-level lowering are displayed in the upper left corner.

not make much difference (experiment G4, Table 4). It should however be noted that only the effects of changing precipitation caused by a constant background temperature change ($T_E = 0$ in Eq. (6)) were tested and that the experiments did not take into account the potential effects of changing precipitation patterns. Such effects would play most at the margin, and therefore the sensitivity tests may not cover the full range of possible behaviour.

Interestingly, when the precipitation sensitivity to temperature is now considered to be the fixed quantity (at 7.3%°C^{-1}), but low and high temperature scenarios

are enforced, the resulting LGM volumes are almost identical (experiments G9 and G10, Table 4). This means that the effects of lower temperatures and lower accumulation rate are largely compensating one another for most of the glacial period and at the LGM. During the Eemian, on the other hand, the effect of the higher temperatures is dominant and cannot be compensated by increased precipitation rates, partly because the rain fraction also increases.

6. Summary and conclusions

In this paper the results were discussed of glacial cycle simulations of the Greenland and Antarctic ice sheets with comprehensive models that account for the most essential features of ice-dynamics, thermodynamics, and glacial isostasy. These experiments were forced by climatic changes derived from ice and sediment cores based on transfer functions that incorporate the best of our current knowledge. In general, the models were shown to reproduce many of the features of the current Greenland and Antarctic ice sheets and their past evolution as evident from available glacial-geological observations. However, the field evidence is still poor in many places and present data do not yet seem to permit conclusive testing, especially concerning thickness changes and aspects of the timing of Holocene retreat.

A particularly sensitive period concerned the Last Interglacial period (Eemian) during which the climate was several degrees warmer than today. Between 123 and 120 kyr BP, the models indicate a Greenland minimum that produced a sea-level rise of $+5.5$ m and an Antarctic minimum equivalent to $+1.4$ m. Interestingly, these numbers combined explain almost exactly the Eemian high stand of 6 m at 122 kyr BP as inferred from the SPECMAP isotope data. This helps to validate the reference model runs as no other ice masses could have been responsible for the inferred global sea-level rise. However, the calculations also brought to light that the Greenland minimum is not very strongly constrained. For plausible combinations of climatic conditions and only small shifts in the duration and magnitude of the peak warming, the ice sheet could have varied from just a little smaller than today to only a small single dome covering only central-north Greenland.

During the LGM, the model predicts that the Antarctic ice sheet expanded close to the continental shelf break almost everywhere. Volume changes were largely concentrated in the West Antarctic and Peninsula ice sheets, and were mainly controlled by global sea-level variations and dynamic processes in the ice shelves. The role of sea level is particularly interesting and supports the view that the Antarctic ice sheet follows events on the northern hemisphere continents by oceanic teleconnections. Except in the Amery Basin, seaward changes of the East Antarctic ice sheet occurred over only small distances. Ice over much of the East Antarctic plateau was generally thinner than today by up to 100 m and varied mainly in accordance with accumulation fluctuations. This is similar to the situation for the Greenland ice sheet, which had a thinning of the central dome by up to several hundred meters at the LGM because of the lower accumulation rates. During that time, the Greenland ice sheet extended beyond the present coastline to cover at least the inner continental shelf, resulting in a coastal belt of ice thickening of on average 1 km thick. Melting was important only during interglacial periods causing the ice sheet to retreat over land.

By varying crucial parameters within their ranges of uncertainty, it is found that corresponding sea-level depressions at 21 kyr BP were comprised between 13 and 21 m for the Antarctic ice sheet and between 1.9 and 3.5 m for the Greenland ice sheet, with best estimates of, respectively, 17.5 and 2.7 m. Given the climatic constraints from ice cores and the marine constraints on their maximum extent, it is therefore hard to conceive that both ice sheets could have contributed more than ca. 25 m of equivalent sea level at the time of maximum sea-level depression. Moreover, the Antarctic estimate probably represents an upper bound because the model does not include a special treatment for individual ice streams or for ice resting on a soft bed. If extensive ice-stream flow comparable to the present Siple Coast continued to exist at the LGM, then WAIS surface elevations may have been substantially lower than simulated by the current model, implying a lower contribution to the total sea-level depression by perhaps several meters. It is expected that the interpretation of ice cores drilled in the vicinity of the Ross and Ronne-Filchner ice shelves will be critical to further resolve this issue. The implication is that the other northern hemisphere ice sheets must have contained an equivalent sea-level volume of between minimum 100 m and perhaps as much as 120 m at the LGM, substantially more than often assumed.

A final point that needs to be stressed concerns the important phase shift of the volume maxima with respect to the commonly accepted period of maximum sea-level depression between 23 and 19 kyr BP. According to the experiments, this maximum was only reached by 16.5 kyr BP for the Greenland ice sheet and by 10 kyr BP for the Antarctic ice sheet, equal to an additional eustatic sea-level lowering of, respectively, 0.4 and 3.7 m. This time lag with respect to melting of ice elsewhere reflects the polar position of both ice sheets causing precipitation increases to dominate over a shrinking domain early during the glacial–interglacial transition. Holocene retreat was essentially complete by 5 kyr BP in Greenland, but is found to still continue today in West

Antarctica before reversing to growth during the next millenium due to delayed isostatic rebound.

References

Ackert Jr., R.P., Barclay, D.J., Borns Jr., H.W., Calkin, P.E., Kurz, M.D., Fastook, J.L., Steig, E.J., 1999. Measurements of past ice sheet elevations in interior West Antarctica. Science 286, 276–280.

Anderson, J.B., 1999. Antarctic Marine Geology. Cambridge University Press, Cambridge, 289pp.

Andrews, J.T., 1992. A case of missing water. Nature 358, 281.

Bentley, M.J., 1999. Volume of Antarctic ice at the Last Glacial Maximum, and its impact on global sea level change. Quaternary Science Reviews 18, 1569–1595.

Bentley, M.J., Anderson, J.B., 1998. Glacial and marine geological evidence for the ice sheet configuration in the Weddell Sea-Antarctic Peninsula region during the Last Glacial Maximum. Antarctic Science 10, 309–325.

Bindschadler, R.A., 1998. Future of the West Antarctic Ice Sheet. Science 282, 428–429.

Blunier, T., Chappellaz, J., Schwander, J., Dällenbach, A., Stauffer, B., Stocker, T.F., Raynaud, D., Jouzel, J., Clausen, H.B., Hammer, C.U., Johnsen, S.J., 1998. Asynchrony of Antarctic and Greenland climate change during the last glacial period. Nature 394, 739–743.

Bromwich, D.H., 1988. Snowfall in High Southern Latitudes. Reviews of Geophysics 26, 149–168.

Clapperton, C.M., Sugden, D.E., 1982. Late Quaternary glacial history of George VI Sound Area, West Antarctica. Quaternary Research 18, 243–267.

Clark, P.U., Mix, A.C., 2000. Ice sheets by volume. Nature 406, 689–690.

Clausen, H.B., Gundestrup, N.S., Johnsen, S.J., Bindschadler, R.A., Zwally, H.J., 1988. Glaciological investigations in the Crête area, Central Greenland. A search for a new drilling site. Annals of Glaciology 10, 10–15.

Colhoun, E.A., Mabin, M.C.G., Adamson, D.A., Kirk, R.M., 1992. Antarctic ice volume and contribution to sea-level fall at 20,000 yr BP from raised beaches. Nature 358, 316–319.

Conway, H.W., Hall, B.L., Denton, G.H., Gades, A.M., Waddington, E.D., 1999. Past and future grounding-line retreat of the West Antarctic ice sheet. Science 286, 280–286.

Cuffey, K.M., 2000. Methodology for use of isotopic climate forcings in ice sheet models. Geophysical Research Letters 27, 3065–3068.

Cuffey, K.M., Clow, G.D., 1997. Temperature, accumulation, and ice sheet elevation in central Greenland through the last deglacial transition. Journal of Geophysical Research 102, 26383–26396.

Cuffey, K.M., Marshall, S.J., 2000. Substantial contribution to sea-level rise during the last interglacial from the Greenland ice sheet. Nature 404, 591–594.

Dahl-Jensen, D., Johnsen, S.J., Hammer, C.U., Clausen, H.B., Jouzel, J., 1993. Past accumulation rates derived from observed annual layers in the GRIP ice core from Summit, Central Greenland. In: Peltier, W.R. (Ed.), Ice in the Climate System, NATO ASI Series, I12, pp. 517–532.

Dahl-Jensen, D., Mosegaard, K., Gundestrup, N.S., Clow, G.D., Johnsen, S.J., Hansen, A.W., Balling, N., 1998. Past temperatures directly from the Greenland ice sheet. Science 282, 268–271.

Dansgaard, W., Johnsen, S.J., Clausen, H.B., Dahl-Jensen, D., Gundestrup, N.S., Hammer, C.U., Hvidberg, C.S., Steffensen, J.P., Sveinbjoernsdottir, A.E., Jouzel, J., Bond, G.C., 1993. Evidence for general instability of past climate from a 250-kyr ice-core record. Nature 364, 218–220.

Denton, G.H., Bockheim, J.G., Wilson, S.C., Stuiver, M., 1989. Late Wisconsin and early Holocene glacial history, Inner Ross Embayment, Antarctica. Quaternary Research 31, 151–182.

Denton, G.H., Hughes, T.J., 1981. The Last Great Ice Sheets. Wiley, New York, 485pp.

Denton, G.H., Hughes, T.J., Karlén, W., 1986. Global ice-sheet system interlocked by sea level. Quaternary Research 26, 3–26.

Elverhøi, A., 1981. Evidence for a late Wisconsin glaciation of the Weddell Sea. Nature 293, 641–642.

England, J., 1999. Coalescent Greenland and Innuitian ice during the Last Glacial Maximum: revising the quaternary of the Canadian High Arctic. Quaternary Science Reviews 18, 421–456.

Fairbanks, R.G., 1989. A 17,000 year glacio-eustatic sea level record: influence of glacial melting rates on Younger Dryas event and deep ocean circulation. Nature 342, 637–642.

Fortuin, J.P.F., Oerlemans, J., 1990. Parameterisation of the annual surface temperature and mass balance of Antarctica. Annals of Glaciology 14, 78–84.

Funder, S., 1989. Quaternary Geology of the Ice-Free Areas and Adjacent Shelves of Greenland. In: Fulton, R.J. (Ed.), Quaternary Geology of Canada and Greenland. Geological Survey of Canada, Ottawa, pp. 743–791.

Funder, S., Hjort, C., Landvik, J.Y., Nam, S., Reeh, N., Stein, R., 1998. History of a stable ice margin—East Greenland during the middle and upper Pleistocene. Quaternary Science Reviews 17, 77–123.

Goodwin, I.D., 1993. Holocene deglaciation, sea-level change, and the emergence of the Windmill Islands, Budd Coast, Antarctica. Quaternary Research 40, 70–80.

Greve, R., 1997. Application of a polythermal three-dimensional ice sheet model to the Greenland ice sheet: response to steady-state and transient climate scenarios. Journal of Climate 10, 901–918.

Grootes, P.M., Stuiver, M., 1986. Ross ice shelf oxygen isotopes and West Antarctic climate history. Quaternary Research 26, 49–67.

Grosfeld, K., Gerdes, R., 1998. Circulation beneath the Filchner ice shelf, Antarctica, and its sensitivity to changes in the oceanic environment: a case-study. Annals of Glaciology 27, 99–104.

Huybrechts, P., 1990. The Antarctic ice sheet during the last glacial–interglacial cycle: a three dimensional experiment. Annals of Glaciology 11, 52–59.

Huybrechts, P., 1992. The Antarctic ice sheet and environmental change: a three-dimensional modeling study. Bremerhaven: Alfred-Wegener-institut für polar-und meeresforschung. Berichte zur Polarforschung 99, 241.

Huybrechts, P., 1994. The present evolution of the Greenland ice sheet: an assessment by modelling. Global and Planetary Change 9, 39–51.

Huybrechts, P., 1996. Basal temperature conditions of the Greenland ice sheet during the glacial cycles. Annals of Glaciology 23, 226–236.

Huybrechts, P., de Wolde, J., 1999. The dynamic response of the Greenland and Antarctic ice sheets to multiple-century climatic warming. Journal of Climate 12, 2169–2188.

Huybrechts, P., Steinhage, D., Wilhelms, F., Bamber, J.L., 2000. Balance velocities and measured properties of the Antarctic ice sheet from a new compilation of gridded datasets for modeling. Annals of Glaciology 30, 52–60.

Imbrie, J.Z., Hays, J.D., Martinson, D.G., MacIntyre, A., Mix, A.C., Morley, J.J., Pisias, N.G., Prell, W.L., Shackleton, N.J., 1984. The orbital theory of Pleistocene climate: support from a revised chronology of the marine $\delta^{18}O$ record. In: Berger, A., Imbrie, J.Z., Hays, J.D., Kukla, G., Saltzman, B. (Eds.), Milankovitch and Climate. D. Reidel, Dordrecht, pp. 269–305.

Ingolfsson, O., Hjort, C., Berkman, P.A., Björck, S., Colhoun, E.A., Goodwin, I.D., Hall, B.L., Hirakawa, K., Melles, M., Möller, P., Prentice, M.L., 1998. Antarctic glacial history since the Last Glacial Maximum: an overview of the record on land. Antarctic Science 10, 326–344.

Jacobs, S.J., Hellmer, H.H., Doake, C.S.M., Jenkins, A., Frolich, R.M., 1992. Melting of ice shelves and the mass balance of Antarctica. Journal of Glaciology 38, 375–387.

Jacobs, S.J., Hellmer, H.H., Jenkins, A., 1996. Antarctic ice sheet melting in the Southeast Pacific. Geophysical Research Letters 23, 957–960.

Janssens, I., Huybrechts, P., 2000. The treatment of meltwater retention in mass-balance parameterizations of the Greenland ice sheet. Annals of Glaciology 31, 133–140.

Jenssen, D., 1983. Elevation and climatic changes from total gas content and stable isotopic measurements. In: de, Q., Robin, G. (Eds.), The Climatic Record in Polar Ice Sheets. Cambridge University Press, Cambridge, pp. 138–144.

Johnsen, S.J., Dansgaard, W., White, J.W.C., 1989. The origin of Arctic precipitation under present and glacial conditions. Tellus 41B, 452–468.

Johnsen, S.J., Dahl-Jensen, D., Dansgaard, W., Gundestrup, N.S., 1995. Greenland palaeotemperatures derived from GRIP bore hole temperature and ice core isotope profiles. Tellus 47B, 624–629.

Jung-Rothenhäusler, F., 1998. Remote sensing and GIS studies in North-East Greenland Bremerhaven: Alfred-Wegener-institut für polar-und meeresforschung. Berichte zur Polarforschung 280, 161.

Kapsner, W.R., Alley, R.B., Shuman, C.A., Anandakrishnan, S., Grootes, P.M., 1995. Dominant influence of atmospheric circulation on snow accumulation in Greenland over the past 18,000 years. Nature 373, 52–54.

Kelly, M., 1985. A review of the Quaternary geology of western Greenland. In: Andrews, J.T. (Ed.), Quaternary Environments Eastern Canadian Arctic, Baffin Bay and Western Greenland. Allen and Unwin, Boston, pp. 461–501.

Koerner, R.M., 1989. Ice core evidence for extensive melting of the Greenland ice sheet in the Last Interglacial. Science 244, 964–968.

Kotlyakov, V.M., Losev, K.S., Loseva, I.A., 1978. The ice budget of Antarctica. Polar Geography and Geology 2 (4), 251–262.

Lang, C., Leuenberger, M., Schwander, J., Johnsen, S.J., 1999. 16°C rapid temperature variation in central Greenland 70,000 years ago. Science 286, 934–937.

Le Meur, E., Huybrechts, P., 1996. A comparison of different ways of dealing with isostasy: examples from modeling the Antarctic ice sheet during the last glacial cycle. Annals of Glaciology 23, 309–317.

Le Meur, E., Huybrechts, P., 1998. Present-day uplift patterns over Greenland from a coupled ice-sheet/visco-elastic bedrock model. Geophysical Research Letters 25, 3951–3954.

Letréguilly, A., Huybrechts, P., Reeh, N., 1991a. Steady-state characteristics of the Greenland ice sheet under different climates. Journal of Glaciology 37, 149–157.

Letréguilly, A., Reeh, N., Huybrechts, P., 1991b. The Greenland ice sheet through the last glacial–interglacial cycle. Palaeogeography, Palaeoclimatology, Palaeoecology 90, 385–394.

Lorius, C., Jouzel, J., Ritz, C., Merlivat, L., Barkov, N.I., Korotkevich, Y.S., Kotlyakov, V.M., 1985. A 150,000-year climatic record from Antarctic ice. Nature 316, 591–596.

Marshall, S.J., Cuffey, K.M., 2000. Peregrinations of the Greenland ice sheet divide in the last glacial cycle: implications for central Greenland ice cores. Earth and Planetary Science Letters 179, 73–90.

Martinerie, P., Lipenkov, V.Y., Raynaud, D., Chappellaz, J., Barkov, N.I., Lorius, C., 1994. Air content paleo record in the Vostok ice core (Antarctica): a mixed record of climatic and glaciological parameters. Journal of Geophysical Research 99, 10565–10576.

Nakada, M., Lambeck, K., 1988. The melting history of the late Pleistocene Antarctic ice sheet. Nature 333, 36–40.

Nicholls, K.W., 1997. Predicted reduction in basal met rates of an Antarctic ice shelf in a warmer climate. Nature 388, 460–462.

Oerter, H., Kipfstuhl, J., Determann, J., Miller, H., Wagenbach, D., Minikin, A., Graf, W., 1992. Evidence for basal marine ice in the Filchner-Ronne ice shelf. Nature 358, 399–401.

Ohmura, A., Reeh, N., 1991. New precipitation and accumulation maps for Greenland. Journal of Glaciology 37, 140–148.

Peltier, W.R., 1994. Ice Age Paleotopography. Science 265, 195–201.

Petit, J.R., Jouzel, J., Raynaud, D., Barkov, N.I., Barnola, J.M., Basile, I., Bender, M., Chappellaz, J., Davis, M.E., Delaygue, G., Delmotte, M., Kotlyakov, V.M., Legrand, M., Lipenkov, V.Y., Lorius, C., Pepin, L., Ritz, C., Saltzman, E., Stievenard, M., 1999. Climate and atmospheric history of the past 420,000 years from the Vostok ice core, Antarctica. Nature 399, 429–436.

Pfeffer, W.T., Meier, M.F., Illangasekare, T.H., 1991. Retention of Greenland runoff by refreezing: implications for projected future sea level change. Journal of Geophysical Research 96, 22117–22124.

Raynaud, D., Whillans, I.M., 1982. Air content of the Byrd core and past changes in the West Antarctic ice sheet. Annals of Glaciology 3, 269–273.

Ritz, C., Fabre, A., Letréguilly, A., 1997. Sensitivity of a Greenland ice sheet model to ice flow and ablation parameters: consequences for the evolution through the last glacial cycle. Climate Dynamics 13, 11–24.

Ritz, C., Rommelaere, V., Dumas, C., 2001. Modeling the Antarctic ice sheet evolution of the last 42,0000 years: implication for altitude changes in the Vostok region. Journal of Geophysical Research, in press.

Robin, G.deQ., 1977. Ice cores and climatic change. Philosophical Transactions of the Royal Society of London Series A 280, 143–168.

Salamatin, A.N., Lipenkov, V.Y., Barkov, N.I., Jouzel, J., Petit, J.R., Raynaud, D., 1998. Ice core age dating and paleothermometer calibration based on istope and temperature profiles from deep boreholes at Vostok Station (East Antarctica). Journal of Geophysical Research 103, 8963–8977.

Severinghaus, J.P., Brook, E.J., 1999. Abrupt climate change at the end of the Last Glacial Period inferred from trapped air in polar ice. Science 286, 930–934.

Solheim, A., Faleide, J.I., Andersen, E.S., Elverhøi, A., Forsberg, C.F., Vanneste, K., Uenzelmann-Neben, G., Channell, J.E.T., 1998. Late Cenozoic seismic stratigraphy and glacial geological development of the East Greenland and Svalbard-Barents Sea continental margins. Quaternary Science Reviews 17, 155–184.

Stuiver, M., Denton, G.H., Hughes, T.J., Fastook, J.L., 1981. History of the marine ice sheet in West Antarctica during the last glaciation: a working hypothesis. In: Denton, G.H., Hughes, T.J. (Eds.), The Last Great Ice Sheets. Wiley, New York, pp. 319–436.

Tushingham, A.M., Peltier, W.R., 1991. Ice-3G: a new global model of Late Pleistocene deglaciation based upon geophysical predictions of post-glacial relative sea level change. Journal of Geophysical Research 96, 4497–4523.

Van de Wal, R.S.W., 1999. The importance of thermodynamics for modeling the volume of the Greenland ice sheet. Journal of Geophysical Research 104, 3887–3898.

Van der Veen, C.J., 1999. Fundamentals of glacier dynamics. A.A. Balkema, Rotterdam, Brookfield, 459pp.

Van Tatenhove, F.G.M., van der Meer, J.J.M., Huybrechts, P., 1995. Glacial geological/geomorphological research in West Greenland used to test an ice-sheet model. Quaternary Research 44, 317–327.

Weidick, A., 1985. Review of glacier changes in West Greenland. Zeitschrift für Gletscherkunde und Glazialgeologie 21, 301–309.

Weidick, A., Oerter, H., Reeh, N., Thomsen, H.H., Thorning, L., 1990. The recession of the inland ice margin during the Holocene climatic optimum in the Jakobshavn Isfjord area of West Greenland. Palaeogeography, Palaeoclimatology, Palaeoecology (Global and Planetary Change Section) 82, 389–399.

Weis, M., Hutter, K., Calov, R., 1996. 25,0000 years in the history of Greenland's ice sheet. Annals of Glaciology 23, 359–363.

Williams, M.J.M., Jenkins, A., Determann, J., 1998. Physical controls on ocean circulation beneath ice shelves revealed by numerical models. In: Jacobs, S.J., Weiss, R.F. (Eds.), Ocean, Ice, and Atmosphere: Interactions at the Antarctic Continental Margin, Vol. 75. American Geophysical Union, Antarctic Research Series, Washington, DC, pp. 285–299.

Yokoyama, Y., Lambeck, K., De Deckker, P., Johnston, P.J., Fifield, L.K., 2000. Timing of the Last Glacial Maximum from observed sea-level minima. Nature 406, 713–716.

Zreda, M., England, J., Phillips, F., Elmore, D., Sharma, P., 1999. Unblocking of the Nares Strait by Greenland and Ellesmere ice-sheet retreat 10,000 years ago. Nature 398, 139–142.